AD-A100 797 AIR FORCE INST OF TECH WRIGHT-PATTERSON AFB OH SCHOO--ETC F/G 9/3
EFFECTS OF A PULSE-FORMING NETWORK OPERATING INTO A NON-LINEAR --ETC(U)
MAR 81 E J KEEFER
UNCLASSIFIED AFIT/GE/EE/81M-4 NL

AD A100797

END
DATE FILMED
7-81
DTIC

DDC

1

LEVEL II

AD A100797

UNITED STATES AIR FORCE

AIR UNIVERSITY

AIR FORCE INSTITUTE OF TECHNOLOGY

Wright-Patterson Air Force Base, Ohio

81 6 30 055

AFIT/GE/EE/81M-4

Accession For	
NTIS GRA&I	X
DTIC TAB	☐
Unannounced	☐
Justification	
By	
Distribution/	
Availability Codes	
Dist	Avail and/or Special
A	

EFFECTS OF A PULSE-FORMING NETWORK

OPERATING INTO A NON-LINEAR LOAD.

THESIS

AFIT/GE/EE/81M-4 Edward J. Keefer, Jr.
2d Lt USAF

Approved for public release; distribution unlimited.

AFIT/GE/EE/81M-4

EFFECTS OF A PULSE-FORMING NETWORK OPERATING INTO A NON-LINEAR LOAD

THESIS

Presented to the Faculty of the School of Engineering
of the Air Force Institute of Technology
Air University
in Partial Fulfillment of the
Requirements for the Degree of
Master of Science

by

Edward J. Keefer, Jr., B.S.
2d Lt USAF
Graduate Electrical Engineering

March 1981

Preface

The purpose of this study was to investigate the effects of a pulse-forming network, within a power modulator, operating into a nonlinear load. This study was part of an Air Force development program at the Air Force Weapons Laboratory, the location for the study's experimental work. The program was canceled late in the study due to a lack of funds, consequently the power modulator was not constructed. Thus, the pulse-forming network's performance within the power modulator was studied only with computer analysis.

For all their help, I would like to thank my advisor Capt F. C. Brockhurst of the Air Force Institute of Technology, Mr. J. P. O'Loughlin of the Air Force Weapons Laboratory, and Mr. M. P. Dougherty and Mr. P. H. Herren of the Air Force Wright Aeronautical Laboratories, Aero Propulsion Laboratory.

Edward J. Keefer, Jr.

Contents

List of Figures

List of Figures

Abstract

The power modulator of an electron-beam gun was computer modeled to investigate the performance of a pulse-forming network (PFN). The PFN was designed for a constant matched load but operated into non-linear load.

The power modulator's operation consisted of: pulsing the electron-beam gun's cathode to a negative 220KV, thru a pulse transformer, by a 50KV hard-tube pulser, this pulser was switched by four parallel power triodes, which were driven by a line-type pulser or PFN. The triodes, the PFN's load, exhibited a non-linear impedance dependent on their grid and plate voltages. The computer model was used to examine the effects of the non-linear load of the power tubes on the PFN.

The PFN was constructed in four; 12KV, 10μsec modules. It was possible to add or remove these modules from the PFN to change the pulse width in 10μsec steps. This modular PFN design was first investigated using a digital computer model and then built and tested for a constant load. Then the effect of operating into a non-linear load was examined by modeling the PFN within the power modulator.

1. Introduction

The Air Force Weapons Laboratory (AFWL) is currently developing pulsed electric discharge lasers (EDL). An indispensable part of an EDL is it's electron-beam gun (E-gun). Hot-cathode electron-beam guns, that are grid controlled, suffer from frequent arc-downs (Ref 7). In order to investigate these cathode-ground breakdowns, AFWL decided to design and build a hot-cathode, grid controlled, electron-beam gun which could accomidate the various experimental studies needed to investigate the breakdown mechanisms.

Considering the E-gun's power requirements, AFWL designed the E-gun's pulse power modulator. The power modulator's operation consisted of: pulsing, thru a pulse transformer, the E-gun's cathode to a negative 220KV by a 50KV hard-tube pulser, this pulser was switched by four power triodes in parallel, which were driven by a line-type pulser or PFN. The PFN consisted of four; 12KV, 10μsec modules. It was possible to add or remove these modules from the PFN to change the pulse width in 10μsec steps.

The laboratory designed the power modulator from prior experience (Ref 8). But it was not possible to anticipate the effect of the non-linear nature of the power tubes, as a load, on the PFN and the power tube - PFN effect on the entire circuit. Without accurate modeling, the circuit behavior could only be determined after testing the completely built circuit.

In this study, the PFN is designed for a matched load. Some non-linear pulsed loads can be described as time-varying resistances. By using Gullemin's method of PFN design it is possible to design voltage-fed networks that will deliver constant voltages to a time-varying resister (Ref 4:189-207). The synthesis procedure requires prior knowledge of the load response for a constant voltage pulse (Ref 1 and 8). The load of the PFN considered varies as the voltage varies at two points, the grid and plate of the power tubes. Thus it was not possible to describe this non-linear load as a time-varying resistor.

The PFN voltage-pulse requirements were dependent on the E-gun voltage-pulse requirements. The breakdown experiments required a voltage-pulse with a 10, 20, 30, or 40 μsec pulse-width at the E-gun's cathode with a rise-time of less than 2μsec, a fall-time of less than 3μsec, and a pulse-plateau ripple of less than 2 per cent. The E-gun voltage-pulse depended on the turn-on and turn-off of the power tubes, which were determined by the PFN voltage-pulse at the tube's grid. Thus the PFN voltage-pulse rise and fall times were critical. The PFN voltage-pulse was to have a rise-time of less than 1μsec and a fall-time of less than 2.5μsec. Once the power tubes had turned on, the E-gun voltage-pulse would be unaffected by any PFN pulse-plateau ripple.

Problem and Scope

The purpose of this study was to investigate the effects of a pulse-forming network, within a power modulator, operating into a non-linear load. The PFN's non-linear load was the driving impedence of the power tubes - a function of the grid and plate voltages. The PFN was designed to meet the modular performance requirements and then constructed for testing. The power modulator, including the power tubes, was then modeled using a digital computer. The non-linear load effect of the power tubes on the PFN was then investigated using computer analysis.

This study was concerned only with the PFN and it's load, the power tubes. The design of the power modulator, the electron-beam gun, or the breakdown experiments were beyond the scope of this project. The scope of this thesis was confined to the design and construction of the PFN, the PFN's inductor coils, the PFN's response to it's load, and the circuit changes to improve that response.

Approach and Presentation

A modular PFN was first designed to operate into a matched load and then applied to a non-linear load. Throughout the study, computer modeling was utilized to investigate the voltage-pulse responses.

The design and testing of the PFN operating into a matched load is presented in Chapter II. The choice of the Rayleigh PFN over the Gullemin Type-E PFN is explained by comparing the voltage-pulse responses of each.

The design and construction of the PFN's inductor coils are covered. The chapter ends with the presentation of the actual test results and a comparison of them to the modeled results.

Chapter III covers the designed PFN operating into the non-linear load of the tubes. The modeling of the power modulator is presented, plus computer results and changes made in the original circuit. A summarization of all the results and the final conclusions and recommendations are made in Chapter IV.

II. The Matched Load Design

The PFN serves the dual purpose of storing the exact amount of energy required for a single pulse and discharging this energy into a load resister R_o in the form of a rectangular pulse. An equivalent model for this pulse discharge is shown in Figure 1, where the PFN is selected so that i(t) approximates a rectangular pulse within an acceptable tolerance when the input voltage v(t) is a step function of amplitude E (Ref 2:4-1).

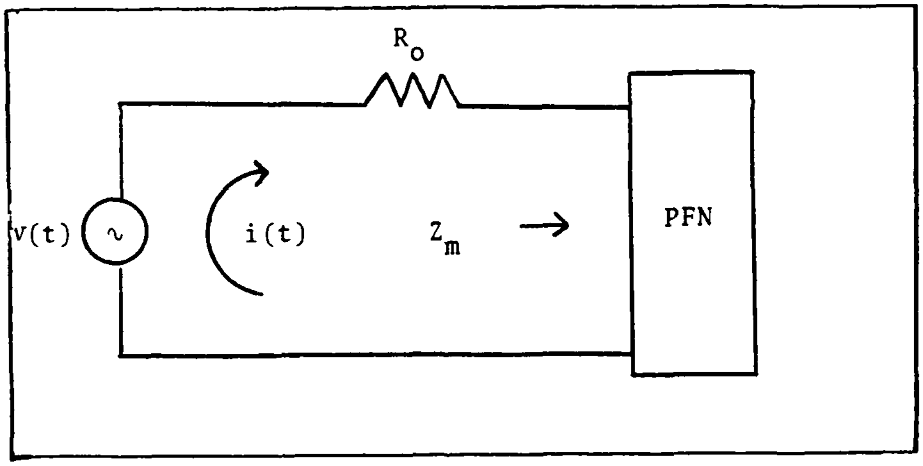

Figure 1. Equivalent Model for Pulse Discharge Current

The ideal PFN is an open-circuited lossless transmission line of characteristic impedance $Z_o = R_o$ and transmission time T/2 where T is the rectangular pulse width. However, practical considerations rule out this line as a PFN, and in

practice this distributed line is simulated by a network composed of a finite number of lumped elements. Although the ideal transmission line yields a flat-top pulse, unavoidable conduction or dielectric losses in the line cause pulse dispersion in the line and droop on the resulting discharge pulse (Ref 2:Chap 4).

The lumped parameter network cannot exactly simulate a distributed transmission line, so an approximation procedure must be employed to determine the network element values. Of the many possible choices for the network, the voltage-fed networks are the most commonly used because only with this type can the usual discharge switches be used. The energy, stored in the electrostatic field of the PFN, is transferred to the load resistor R_o when the discharge device is switched to a conducting state.

Choice of PFN Type

Two voltage-fed network classes were investigated; the Gullemin Type-E network in Figure 2(a), and the Rayleigh network in Figure 2(b). In each network all capacitors are the same. There are other equivalent networks for the Gullemin voltage-fed network, but these networks do not offer any appreciable advantages over the Type-E (Ref 4:201).

The network in Figure 2(b) is the lumped-parameter approximation to the transmission line, truncated after N sections. It is called the Rayleigh network because application of Rayleigh's principle to the transmission line yields this two-terminal line-simulating network (Ref 4:171-185).

The Rayleigh network is well suited for modular separation because each section is identical. The Gullemin Type-E network, because the inductors are not restricted to the same value, produces a better approximation to the rectangular pulse than does the Rayleigh network, for the same number of elements. However, the close interrelationship among element values does not make this network adaptable for modular separation. Furthermore, careful control of the coupling between coils is required.

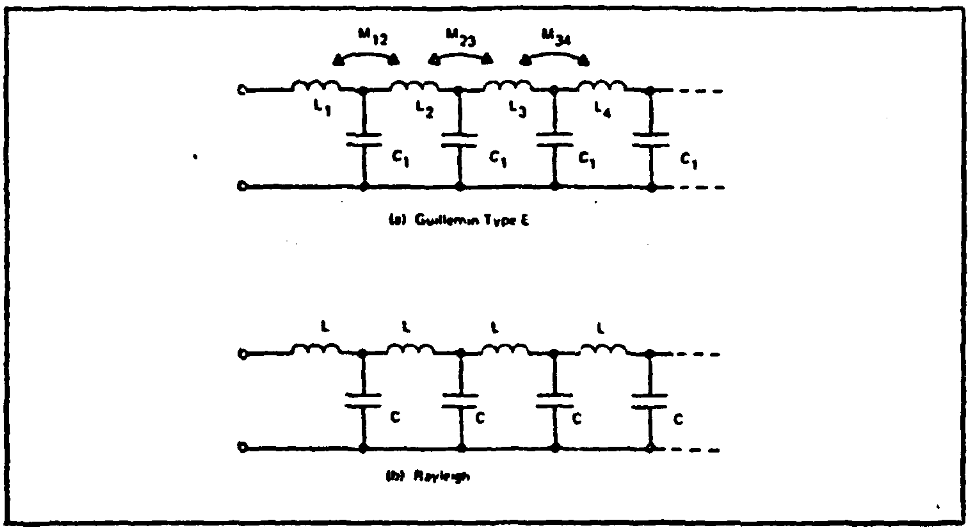

Figure 2. Pulse-Forming Networks that were Examined.

In an effort to meet modular requirements the responses of the Type-E and Rayleigh networks were studied as element values were changed and modules were added and removed. The PFN selected to drive the power tubes was required to have minimum pulse-plateau ripple between modules, a rise time of less than 1μsec, and a fall-time of less than 2.5μsec.

The following PFN designs use a matching impedence of 15 ohms. This is the average impedence "seen" by the PFN. The PFN voltage-pulse is applied to the tube grid through a polarity-reversing pulse transformer (turns ratio 1.2 to 1). The required average grid voltage during the PFN voltage-pulse is 3KV. For an average plate voltage of 5KV, the average grid current will be 120 amps or for four tubes 480 amps (Ref 6). Overcoming a negative 2KV grid bias voltage, the PFN is required to supply an average voltage of 6KV and an average current of 400 amps during the PFN voltage-pulse. This is an average impendence of 15 ohms.

A seven-section Type-E network was designed for a load impedence, R_0=15 ohms and a pulse width, τ=10µsec. The total network inductance and capacitance were equal to

$$L_T = \tau R_0/2 \tag{1}$$

$$C_T = \tau/2R_0 \tag{2}$$

These total values for inductance and capacitance were equally divided among the sections, except for L_1 and L_7 which had 20 per cent more self inductance. The mutual inductance between each coil was equal to 15 per cent of the self inductance of each center section. The network was modeled, using a SCEPTRE program, on a digital computer. The listing of the Type-E program can be seen in Appendix C(Ref 3). The network inductors and the mutual coupling between them were then adjusted to obtain an optimum response. The final network is shown in Figure 3. The voltage-pulse for this network is shown in Figure 4.

The rise-time is 0.7μsec, which is less than the required 1μsec and the fall-time is 1.5μsec, which is less than the required 2.5μsec.

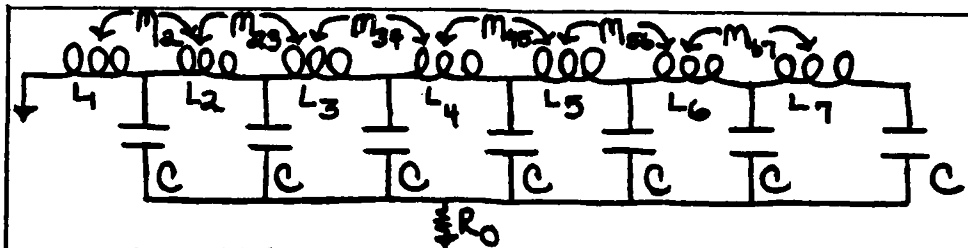

L_1 = 16μh	M_{12} = 1.5μh	C = 50nf
L_2 = 10μh	M_{23} = 1.5μh	R_0 = 15Ω
L_3 = 10μh	M_{34} = 1.5μh	
L_4 = 10μh	M_{45} = 1.5μh	
L_5 = 10μh	M_{56} = 1.5μh	
L_6 = 10μh	M_{67} = 1.2μh	
L_7 = 12μh		

Figure 3. Seven-Section Type-E PFN with a 10μsec pulse width

The affect of adding modules of similar PFNs for longer pulsewidths was then examined. To obtain a satisfactory pulse-plateau ripple the various inductors of a Type-E network are adjusted. This is not possible if modules are added or removed as required. There is also no mutual inductance between the last inductor of one module and the first of an adjoining module. The voltage-pulse waveforms of the network after adding one module is shown in Figure 6, after two modules in Figure 7, and after three modules in Figure 8. Excessive pulse-plateau distortion occurs whenever modules are added or removed because of the lack of mutual inductances between modules.

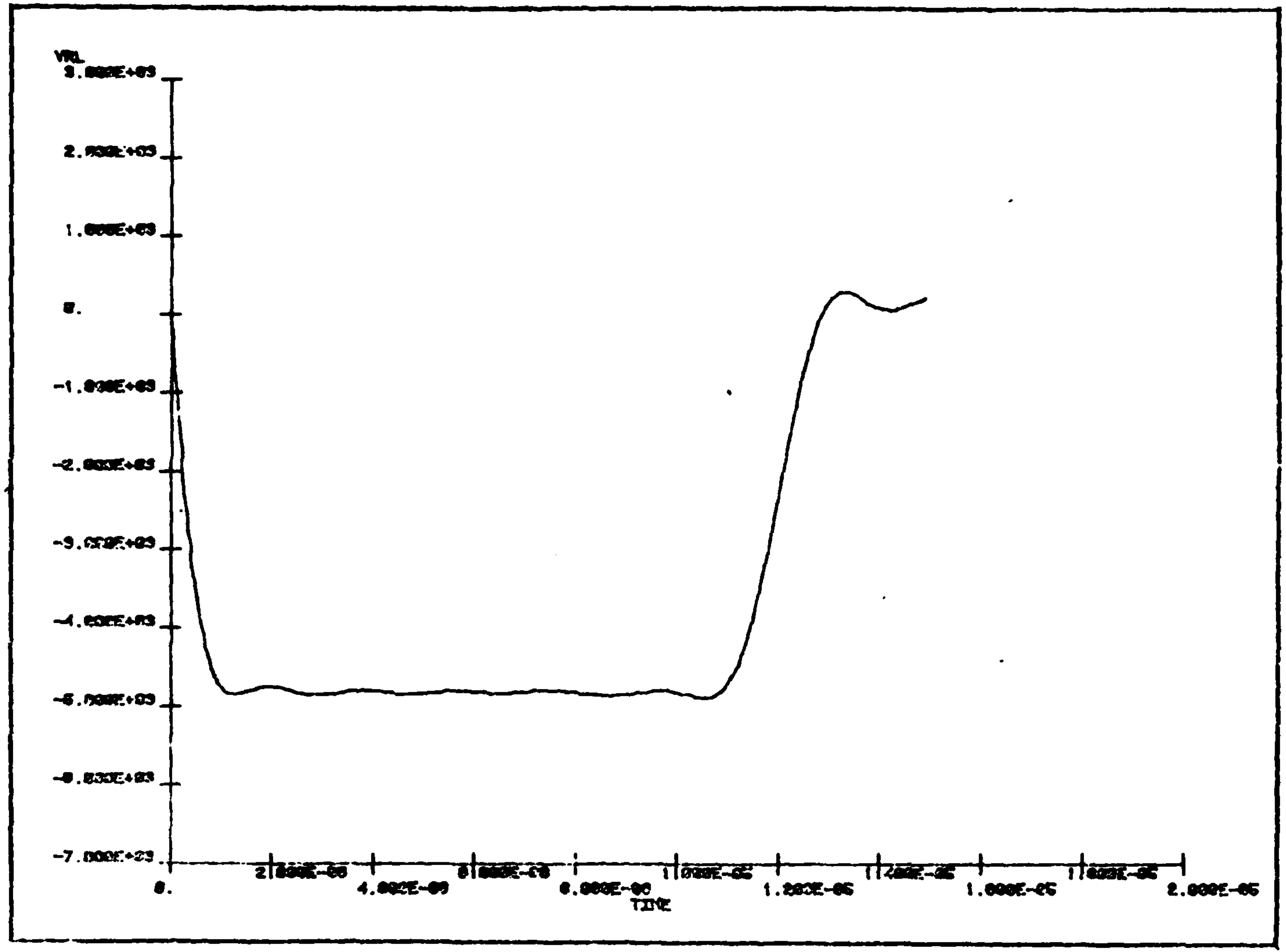

Figure 4. Voltage-Pulse for the Type-E PFN in Figure 3.

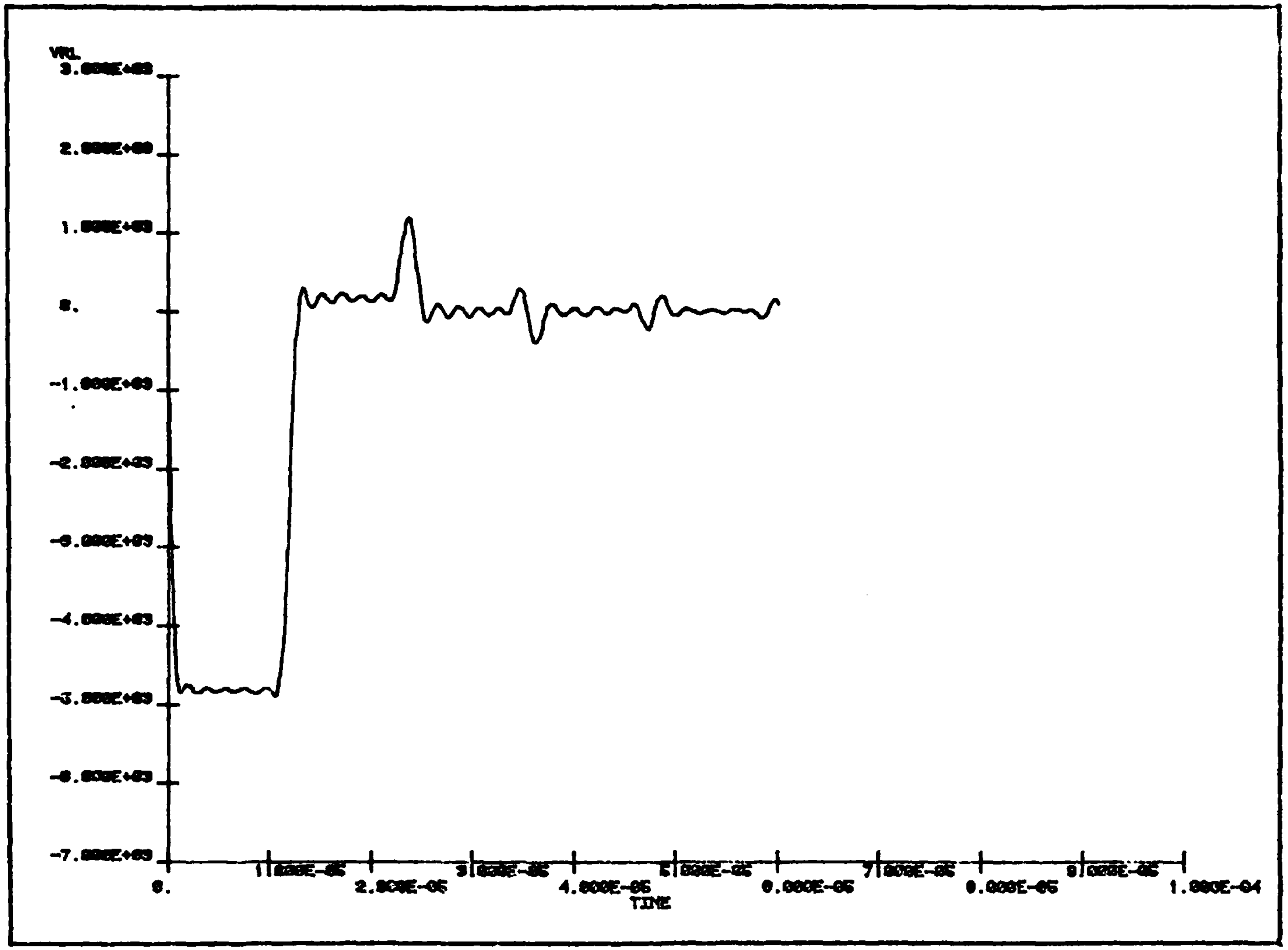

Figure 5. Voltage-Pulse for One Module of a Type-E PFN

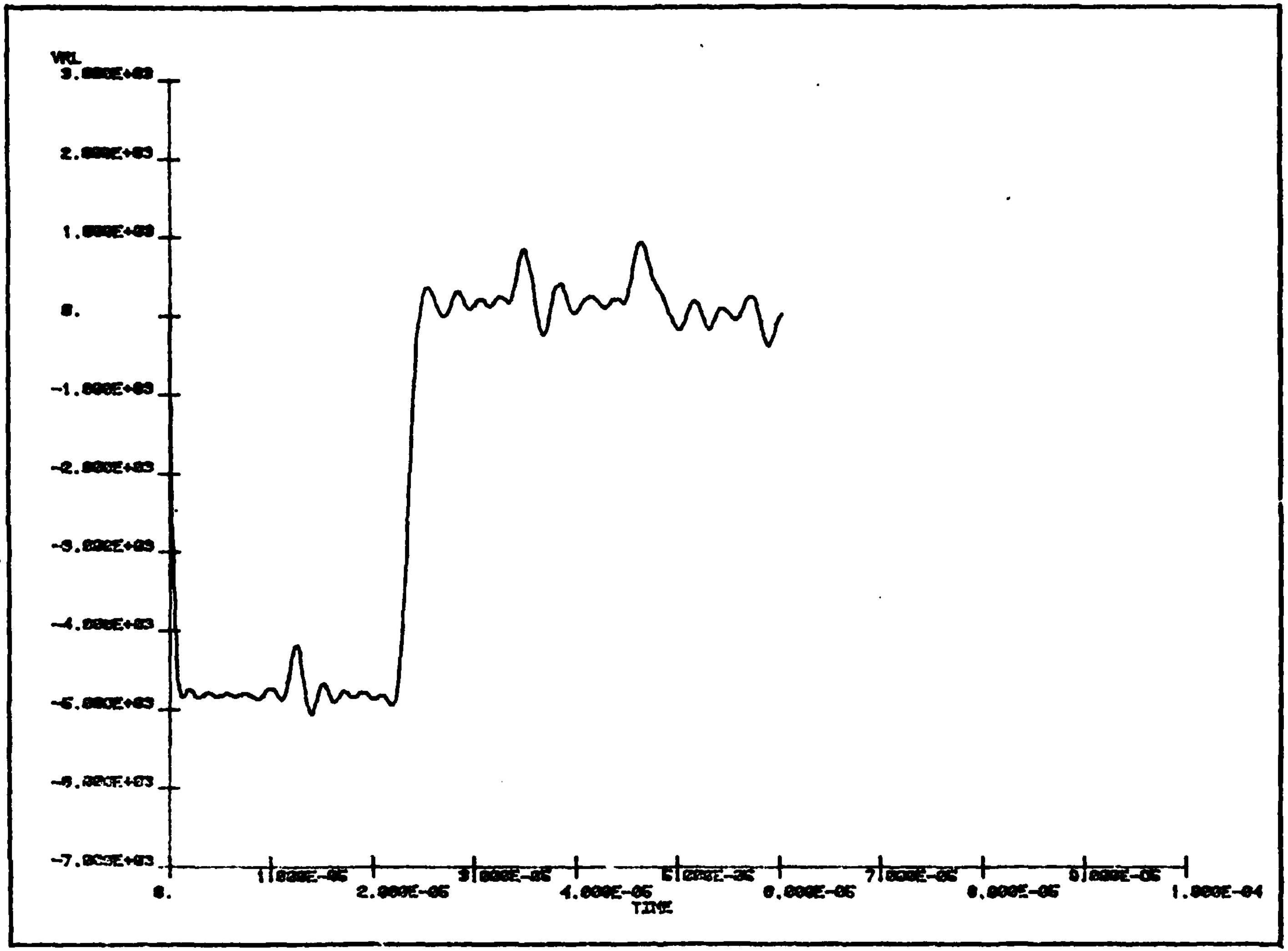

Figure 6. Voltage-Pulse for Two Modules of a Type-E PFN

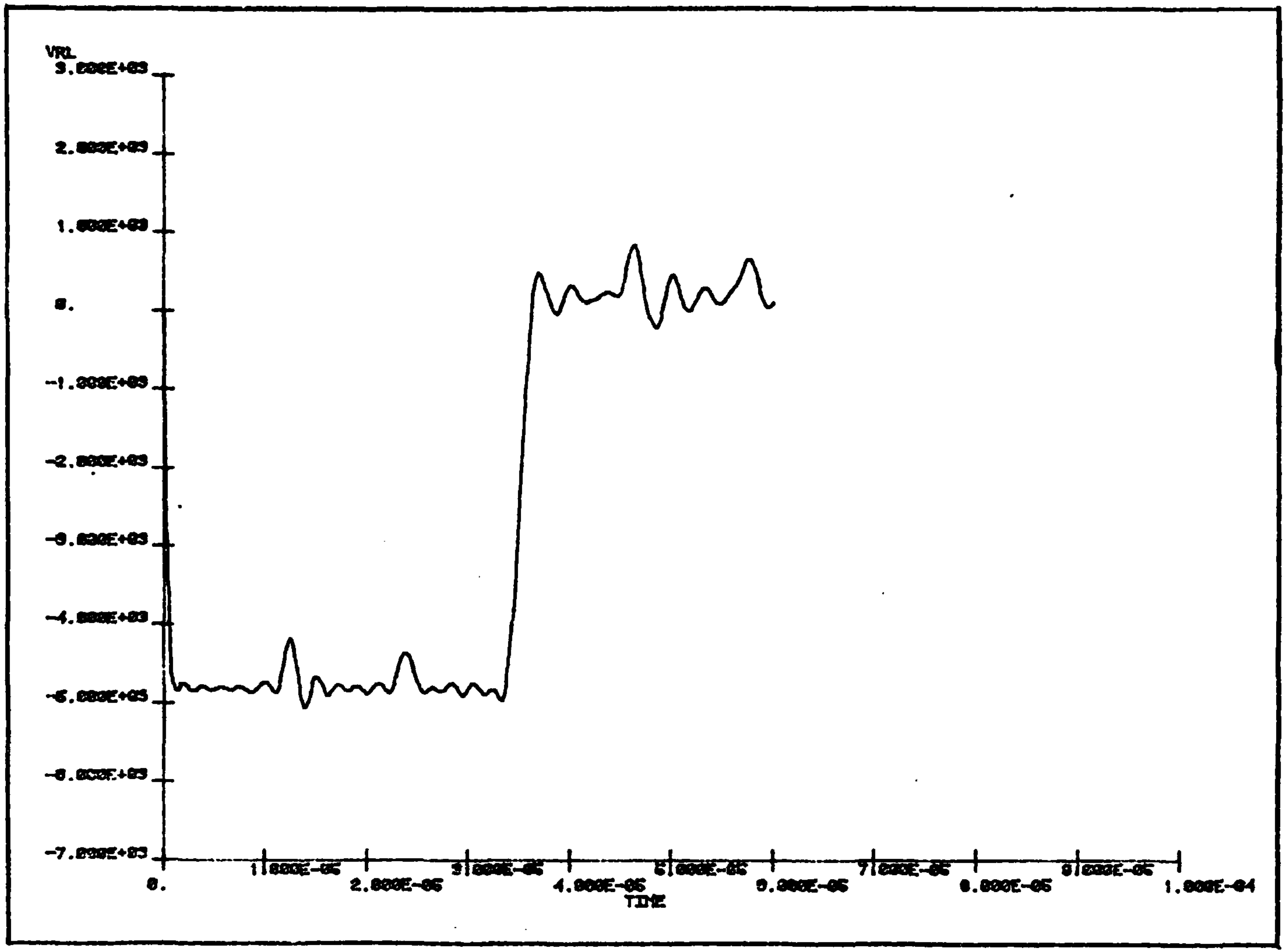

Figure 7. Voltage-Pulse for Three Modules of a Type-E PFN

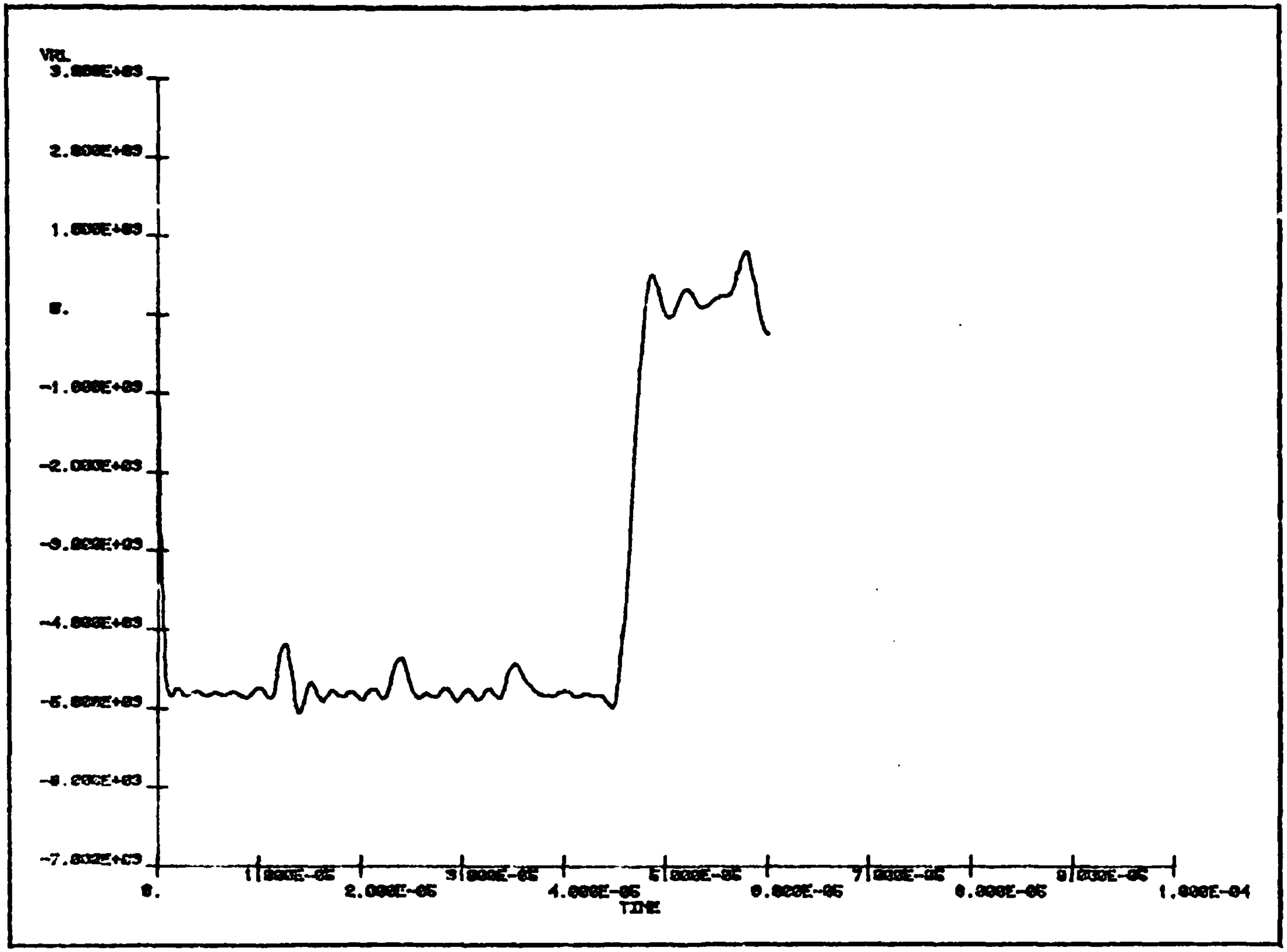

Figure 8. Voltage-Pulse for Four Modules of a Type-E PFN

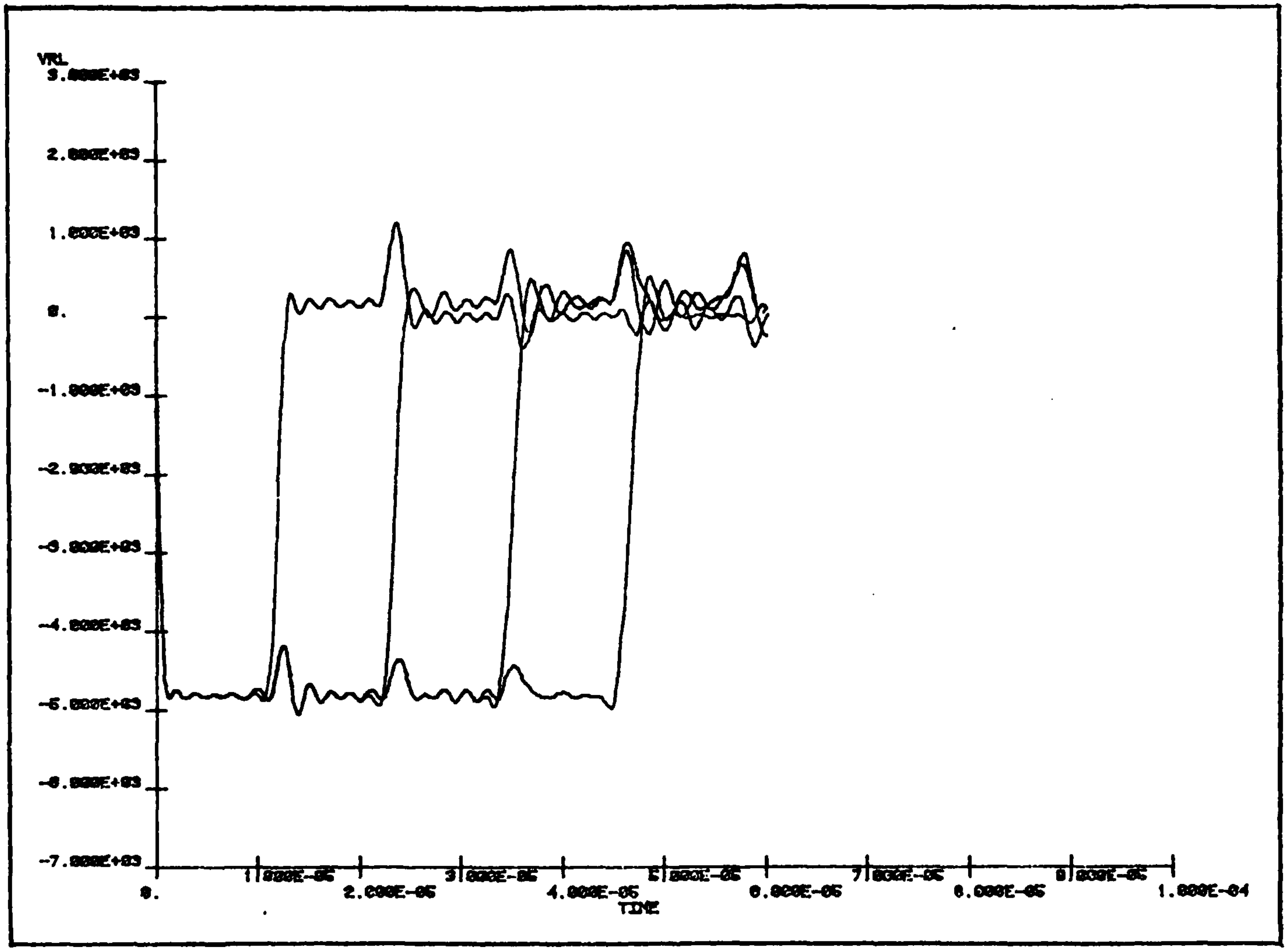

Figure 9. Composite for all Modular Type-E PFN Voltage Pulses

The results in the last paragraph suggested that the requirements of a variable pulsewidth could best be accomplished by having identical modules without mutual inductance between each module. The pulse-width then becomes a function of the number of plug-in modules. This configuration is the Rayleigh network in Figure 2(b), where for N sections

$$L = R_o\ T/2N \tag{3}$$

$$C = T/2NR_o \tag{4}$$

A seven-section Rayleigh PFN was designed for a 10μsec pulse-width and a 15 ohm impedence, yielding L = 11μh and C = 50nf. In order to reduce the overshoot and pulse-plateau ripple the value of the leading inductor was increased to 19μh. Again the circuit was modeled on the digital computer using the SCEPTRE program (the Rayleigh program listing can be seen in Appendix C). The voltage-pulse response is shown in Figure 10. Modules of similar PFNs (except all section inductors are equal) were then added. Figures 11, 12, 13, and 14 show the voltage-pulse responses for one, two, three, and four modules connected, respectively. A compositive of the digital computer responses of this PFN, as identical modules are added, are shown in Figure 15. The pulse-plateau ripples and rise-times remain the same as modules are added. The rise-time was 0.75μsec, which was less than the required 1μsec, and the fall-times were 2.4μsec, which were less than the required fall-time of 3μsec. Because of the excellent modular response of the Rayleigh PFN it was chosen as the power modulator's PFN.

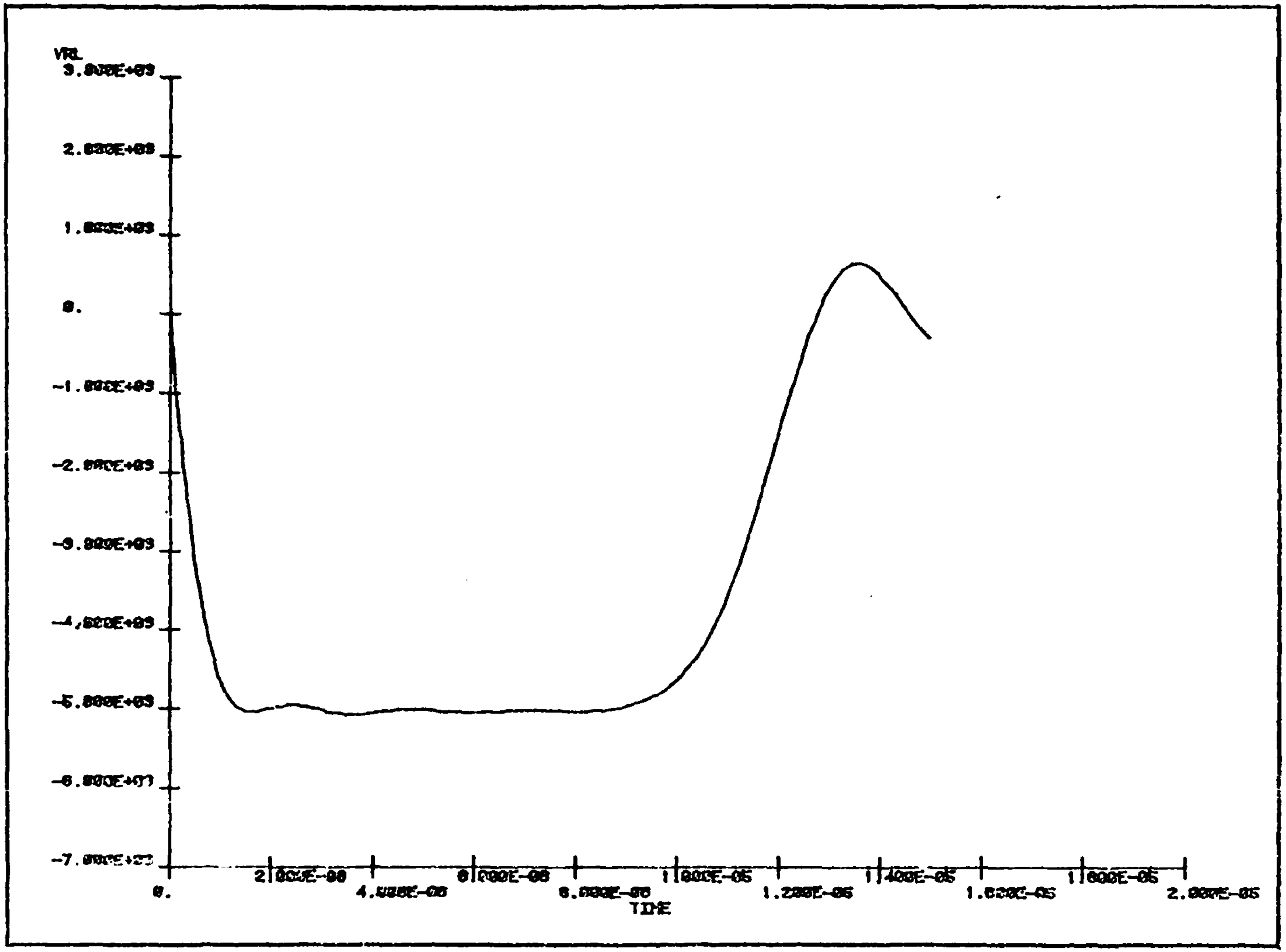

Figure 10 Voltage-Pulse for a Rayleigh PFN

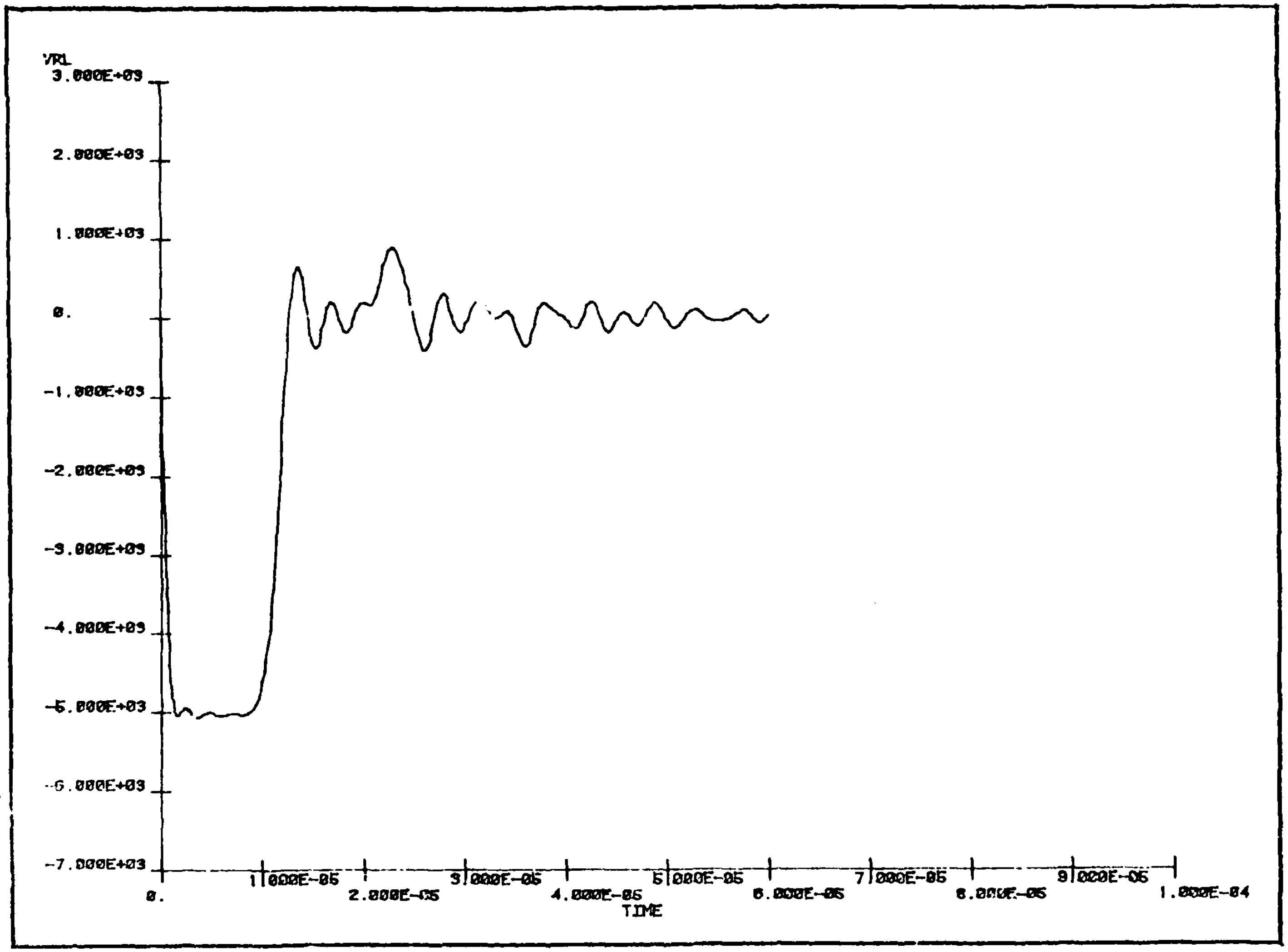

Figure 11. Voltage-Pulse for One Module of a Rayleigh PFN.

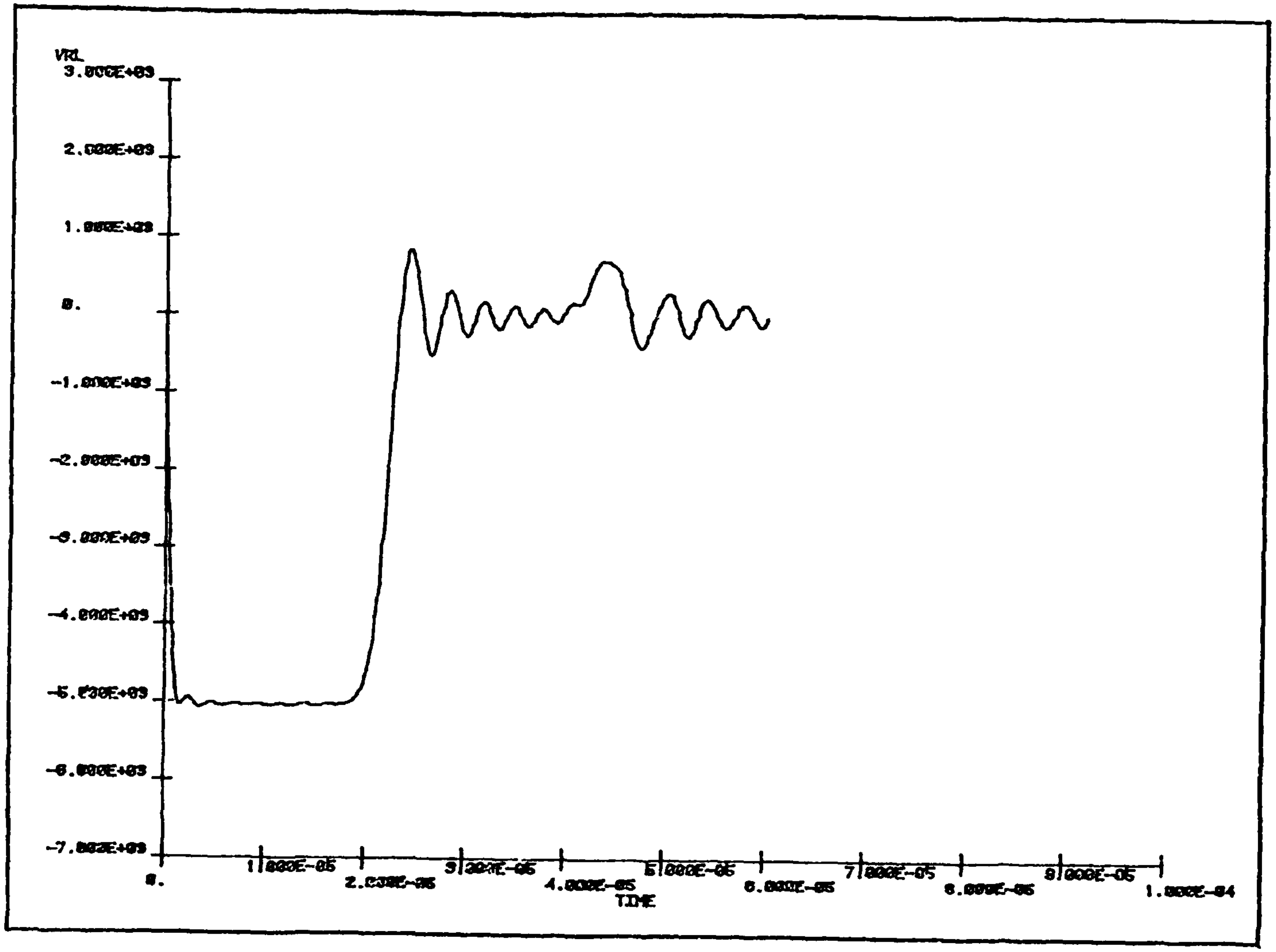

Figure 12. Voltage-Pulse for Two Modules of a Rayleigh PFN

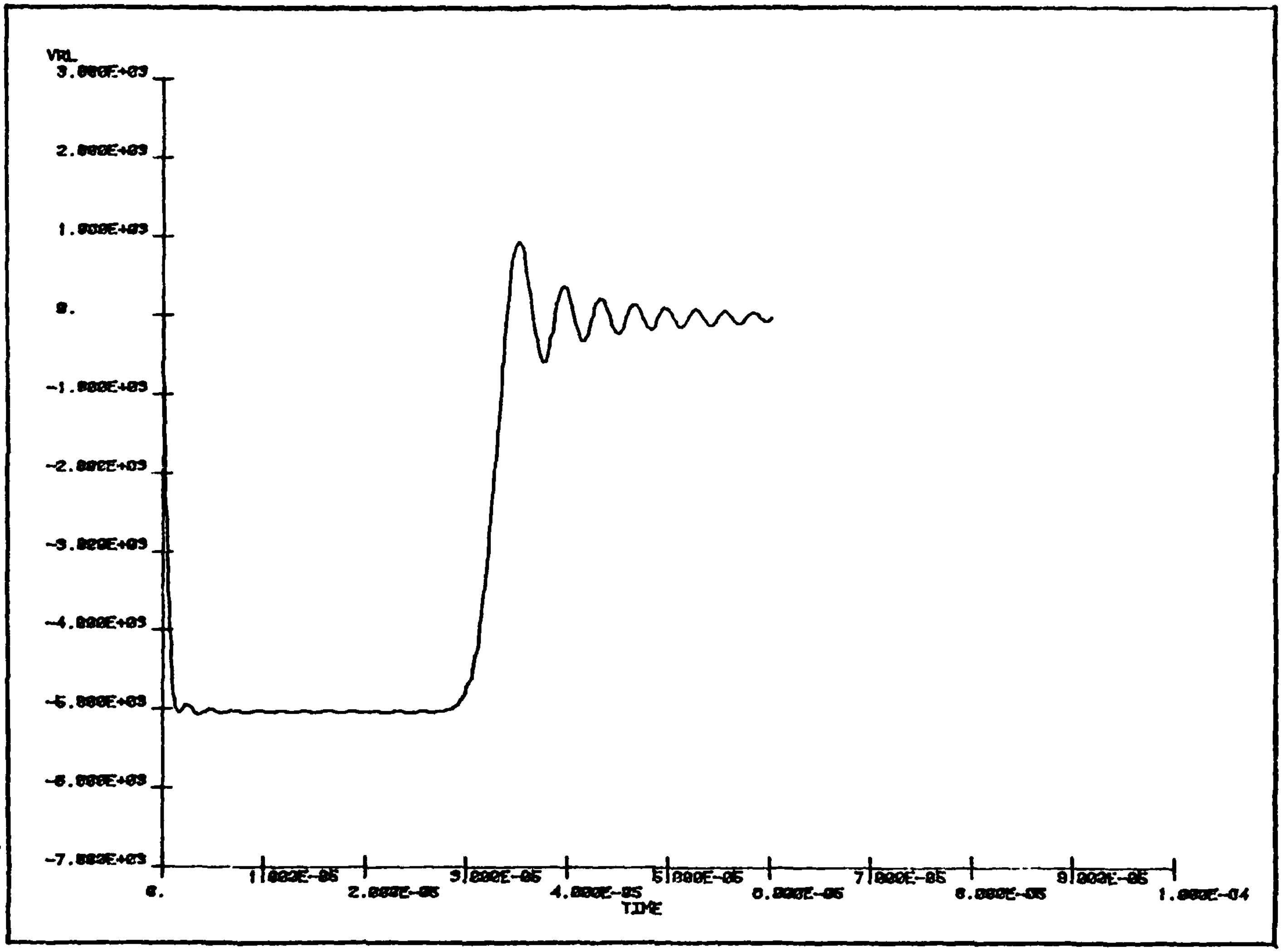

Figure 13 Voltage-Pulse for Three Modulesof a Rayleigh PFN

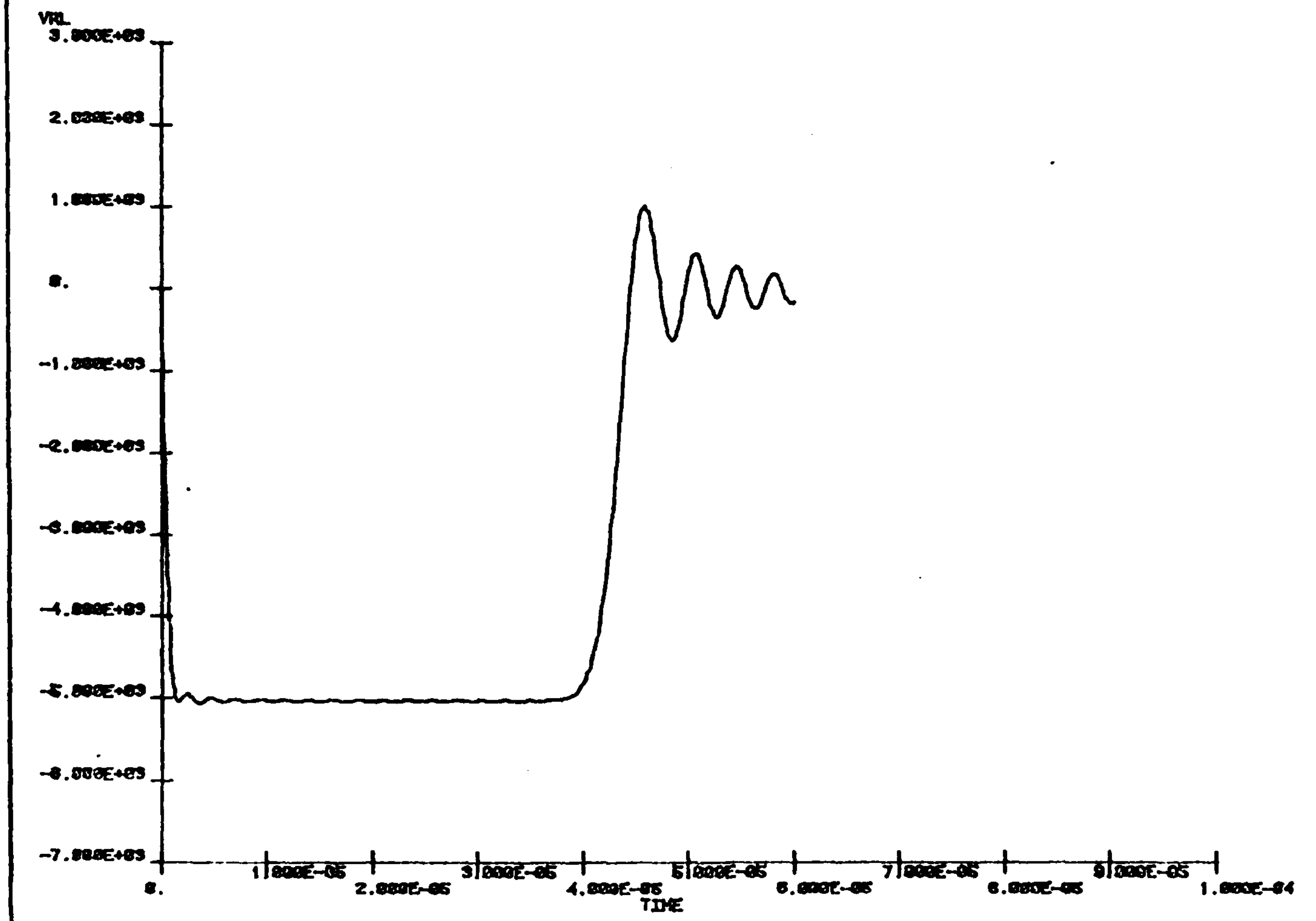

Figure 14. Voltage-Pulse for Four Modules of a Rayleigh PFN

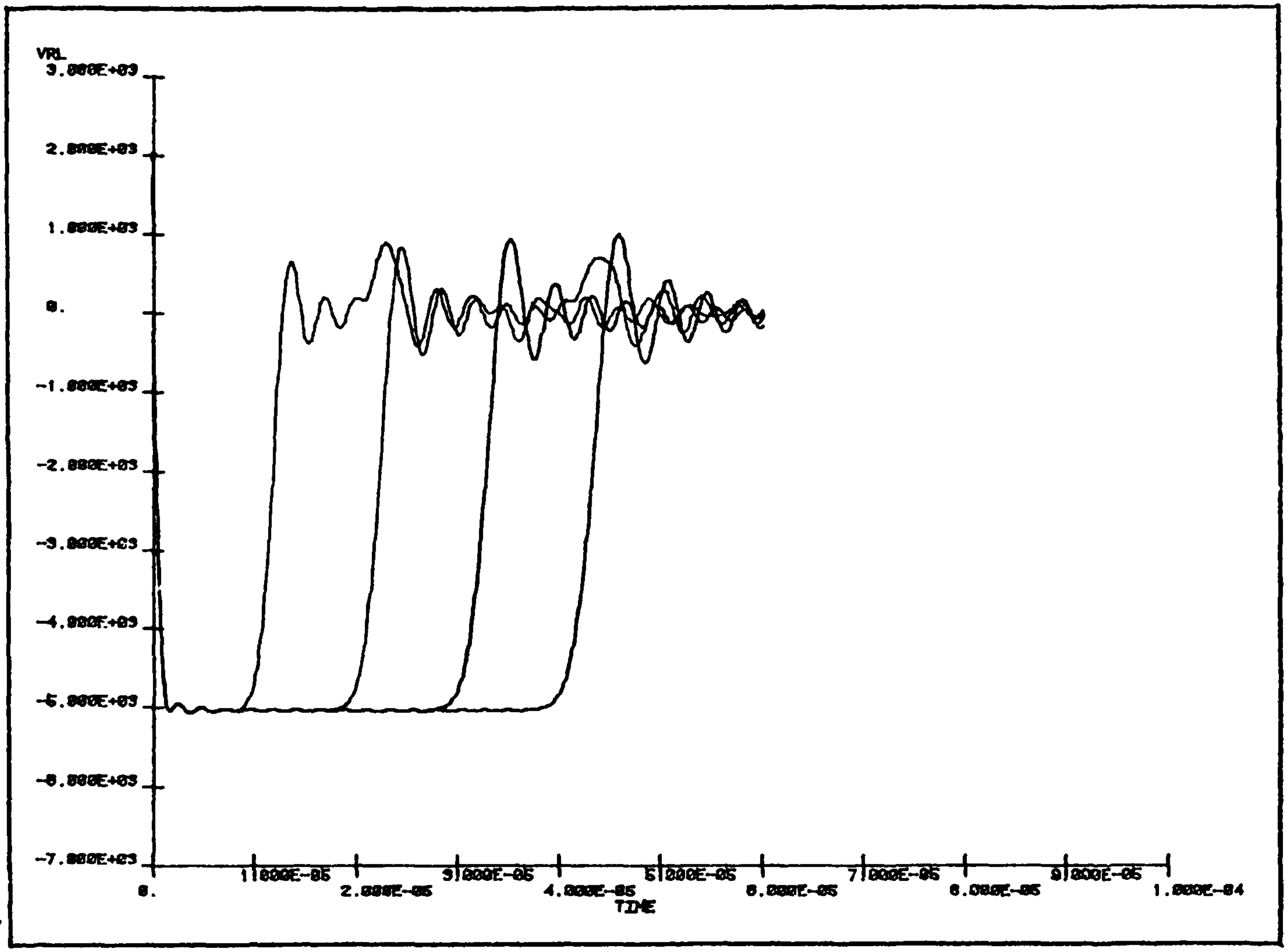

Figure 15. Composite for all Modular Rayleigh PFN Voltage-Pulses

Coil Design and Construction

Because of the excellent modular response of the Rayleigh PFN is was chosen as the power modulator's PFN. The Rayleigh PFN was first studied using computer analysis. The next step was to actually construct a Rayleigh PFN based on that computer analysis.

Since the capacitors were purchased, it was only necessary to design the inductor coils. The main design constraint for the inductors was the operating space the PFN would occupy, a rack measuring 36 inches deep, 36 inches wide, 36 inches high. Using Nagaoka's inductance formula and working within the required space; it was decided to wrap the inductor coils (using number 10 wire) on four and one half inch diameter, thirty six inch long PVC plastic tubes (Ref 5:142-147). The coils were four and three fourths inches long, with a separation of five inches between each coil - to ensure negligible mutual coupling. The coils were open to the air for cooling and so each could be fine tuned by movable taps.

Further information on the coil inductance calculations and the minimization of the mutual inductances can be found in Appendix A and Appendix B.

Test Results

The PFN was tested using 50nf, 400 volt capacitors (the high-voltage capacitors had not yet arrived). The PFN was operated into a matched load of 15 ohms, while modules were added and removed and the voltage-pulse responses were photographed. Figures 16, 17, 18, and 19 show the voltage-pulse

responses for one, two, three, and four modules connected, respectively. A composite of all four responses are shown in the time-lapsed photograph in Figure 20. The pulse-plateau ripples and rise-times remain the same as modules are added and removed. No excessive pulse-plateau distortion occurs. The rise-time was 0.9μsec, which was less than the required 1μsec, and the fall-times were 2.2μsec, which were less than the required fall-time of 3μsec. The pulsewidths were 10, 20, 30, and 40μsec, and were acheived by tuning the inductors.

There is a close correlation between the actual test results and the computer analysis results. Using the computer program SCEPTRE it was possible to model the performance of the Rayleigh and Type-E PFNs on a digital computer. Due to the excellent modular responses of the Rayleigh PFN it was chosen as the power modulator's PFN. A Rayleigh PFN was then optimized using the digital computer. As the actual test results show the computer model was an acurate representation of the Rayleigh PFN.

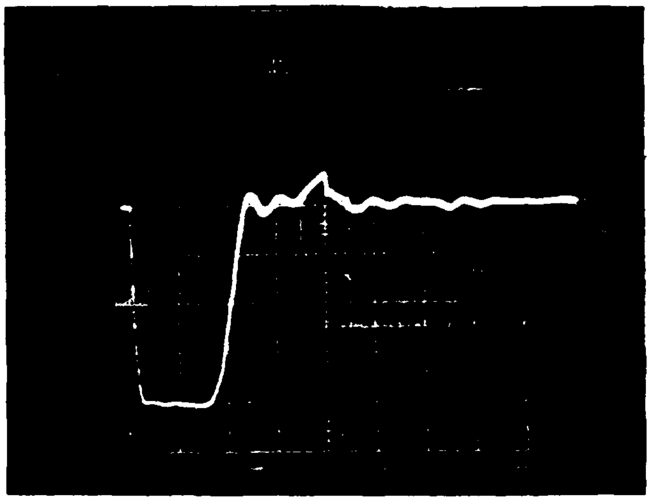

Figure 16 Actual Voltage-Pulse for One Module of a Rayleigh PFN

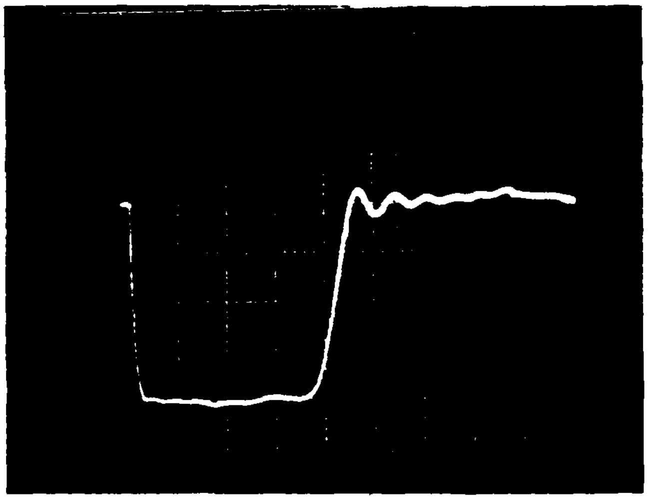

Figure 17 Actual Voltage-Pulse for Two Modules of a Rayleigh PFN

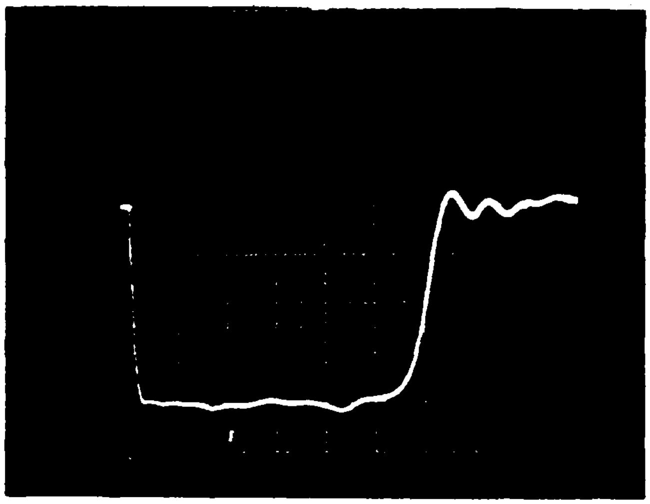

Figure 18 Actual Voltage-Pulse for Three Modules of a Rayleigh PFN.

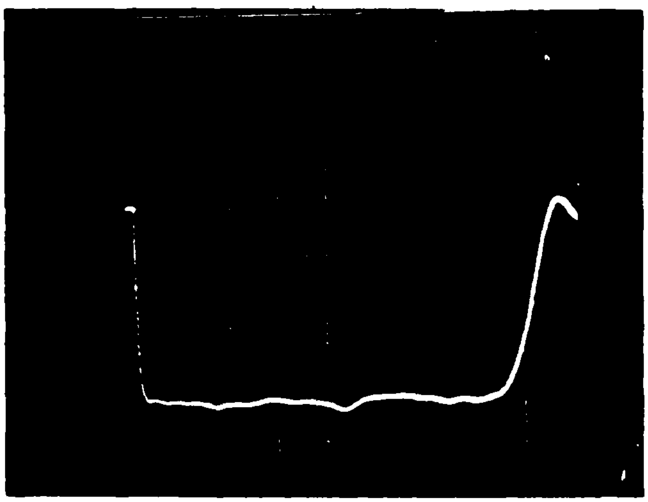

Figure 19 Actual Voltage-Pulse for Four Modules of a Rayleigh PFN

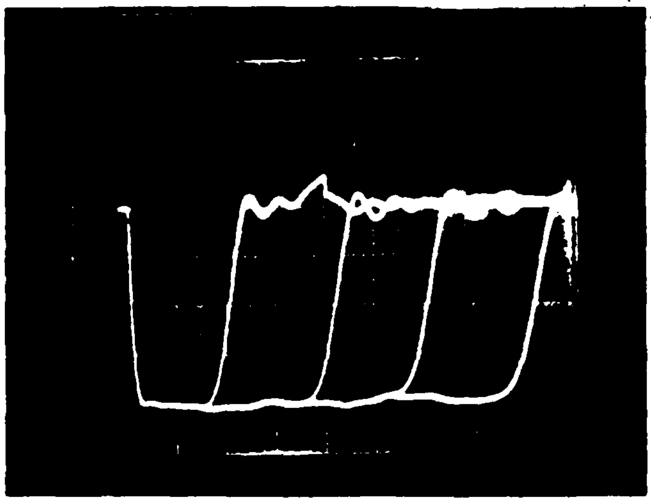

Figure 20 Actual Composite for all Modular Rayleigh PFN Voltage Pulses

III. Operating Into a Non-Linear Load

The power modulator was the power source for the electron-beam gun. The pulse power modulator circuit is shown in Figure 21. The power circuit operation consisted of: pulsing the E-gun's cathode to a negative 220KV thru a pulse transformer with a 50KV hard-tube pulse, this pulser was switched by four parallel power triodes, which were driven by a line-type pulser or PFN. The PFN's non-linear load was the driving impedence of the power tubes, determined by the grid voltage and current - a function of the grid and plate voltages.

Modeling the Power Modulator

The power modulator was modeled by writing a FORTRAN program and then analyzed on a digital computer. The circuit equations were written directly in FORTRAN according to a systematic set of rules developed by AFWL (Ref 9). The circuit analysis method required equations expressing the voltages at every node and the inductive currents flowing into every node. The grid and plate voltages were simply nodal voltages. The grid and plate currents were functions of the grid and plate voltages, so they were determined by subroutines derived from the tube characteristic chart (Ref 6). These equations and subroutines can be seen in the complete FORTRAN program of the power modulator, located in Appendix C.

The completely modeled power circuit is shown in Figure 22. The elements to the left of node V_8 comprise the seven-section PFN reflected to the secondary of the transformer TR4

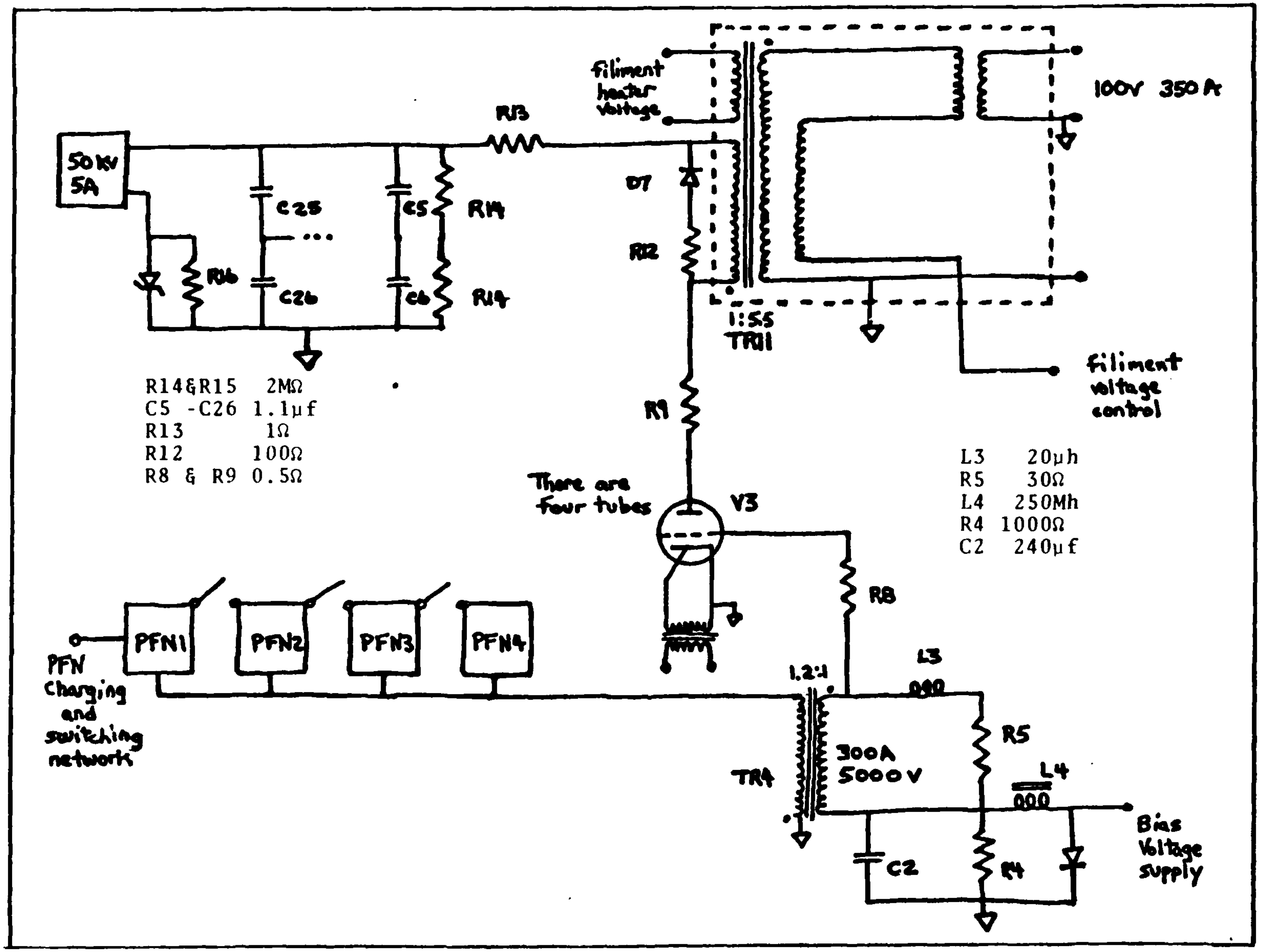

Figure 21. The Pulse Power Modulator Circuit.

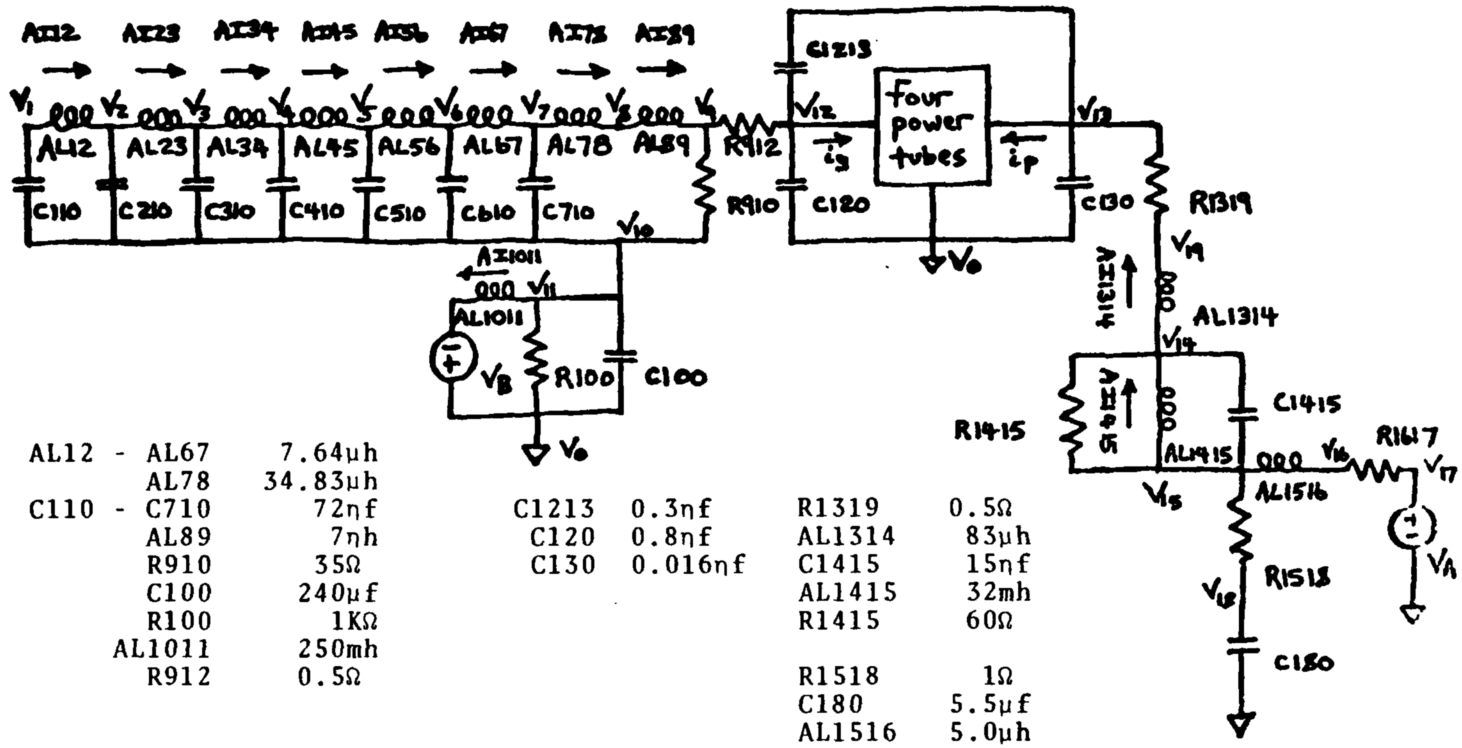

AL12 - AL67	7.64μh
AL78	34.83μh
C110 - C710	72ηf
AL89	7ηh
R910	35Ω
C100	240μf
R100	1KΩ
AL1011	250mh
R912	0.5Ω

C1213	0.3ηf
C120	0.8ηf
C130	0.016ηf

R1319	0.5Ω
AL1314	83μh
C1415	15ηf
AL1415	32mh
R1415	60Ω
R1518	1Ω
C180	5.5μf
AL1516	5.0μh
R1617	100Ω

Figure 22. The Pulse Power Modulator Circuit Model

of Figure 21. AL89 is the calculated leakage inductance of TR4. The PFN charging section of the power circuit is not included in the model. The PFN is initially charged to 10KV, and then discharged. Only one pulse is necessary to study the power circuit's response.

The elements below node 10 comprise the tube biasing section, which maintains a negative 2KV at node 10. This bias voltage ensures the tube will not operate in the negative grid current region. Voltage source, VB represents the rectified voltage supply for the bias section.

The hard-tube pulser is modeled by the elements below and to the right of node 15. Capacitor, C180 is the pulser's total capacitance, and AL1516 represents the total inductance. Voltage source, VA is the pulser's 50KV DC power supply.

The E-gun impedence is represented by R1415, reflected to the primary of TR7 of Figure 21. The calculated leakage inductance of TR7 is AL134. The coil inductance and shunt capacitance of TR7 are C1415 and AL1415. The E-gun impendence was modeled first as a constant and then as an emission limited impendence. For emission limiting the current was limited by a function subroutine which determined an appropriate value of R1415 as a function of the impedence voltage. The emission limiting subroutine derivation is shown in Appendix D.

The grid and plate voltages are at nodes 12 and 13. The inter-electrode capacitances are C1213-from grid to plate, C120-from grid to filament, and C130-from plate to filament (Ref 6). The grid and plate currents, being functions of the tube

voltages, were determined by function subroutines. Linear equations were derived to closely approximate the non-linear relationship (obtained from the tube characteristic curves) between the tube voltages and currents (Ref 6). How these subroutines were derived is shown in Appendix D.

Computer Results

The FORTRAN model made it possible to verify the power modulator design, before it was constucted. The voltage-pulse responses; at the grid and plate of the power tubes, across the E-gun, and at the PFN were studied to improve the overall response.

Modulator elements were varied or removed to obtain a better response. A rise-time peaking inductor, L3 in Figure 21, was found to be unnecessary and removed. Varying the resister R5, in Figure 21, affected the shape of the PFN and grid voltage-pulse responses. The E-gun and plate voltage-pulse responses were affected by the tube turn-on and turn-off, which was determined by the grid voltage.

The PFN and grid voltage-pulse responses, shown in Figures 23 and 24, oscillated at the end of each pulse. While these oscillations did not cause problems in the computer analysis, an effect was made to minimize them since they could cause the tubes to go unstable (due to negative feedback). The plate and E-gun voltage-pulse responses, shown in Figures 24 and 25, did not exhibit these end of pulse oscillations, because the grid oscillations occured after the tube had turned off. Reasons for these oscillations and how they were reduced to their final level are given in the final conclusions, Chapter IV.

Table 1

Voltage-Pulse Parameters for Modeled Pulse Modulator

	E-Gun	Plate	Grid	PFN
Pulse Height(KV)	45.0	5.0	1.0	1.2
Pulse Width (μsec)	13.0	11.0	13.0	1.2
Rise-Time (μsec)	1.8	0.5	1.8	1.3
Fall-Time (μsec)	3.0	0.5	4.0	6.5

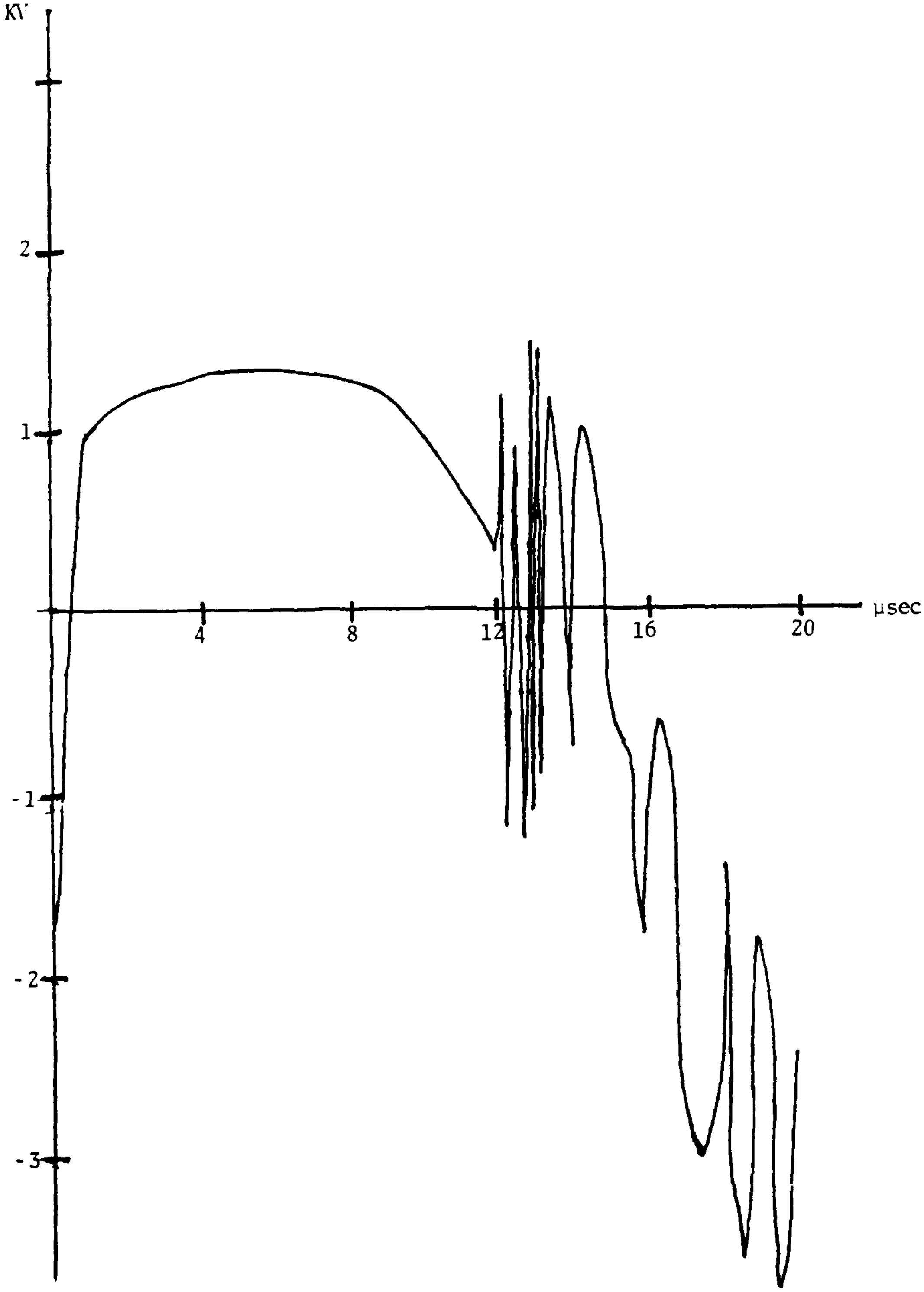

Figure 23. Voltage-Pulse of the PFN Within the Modulator

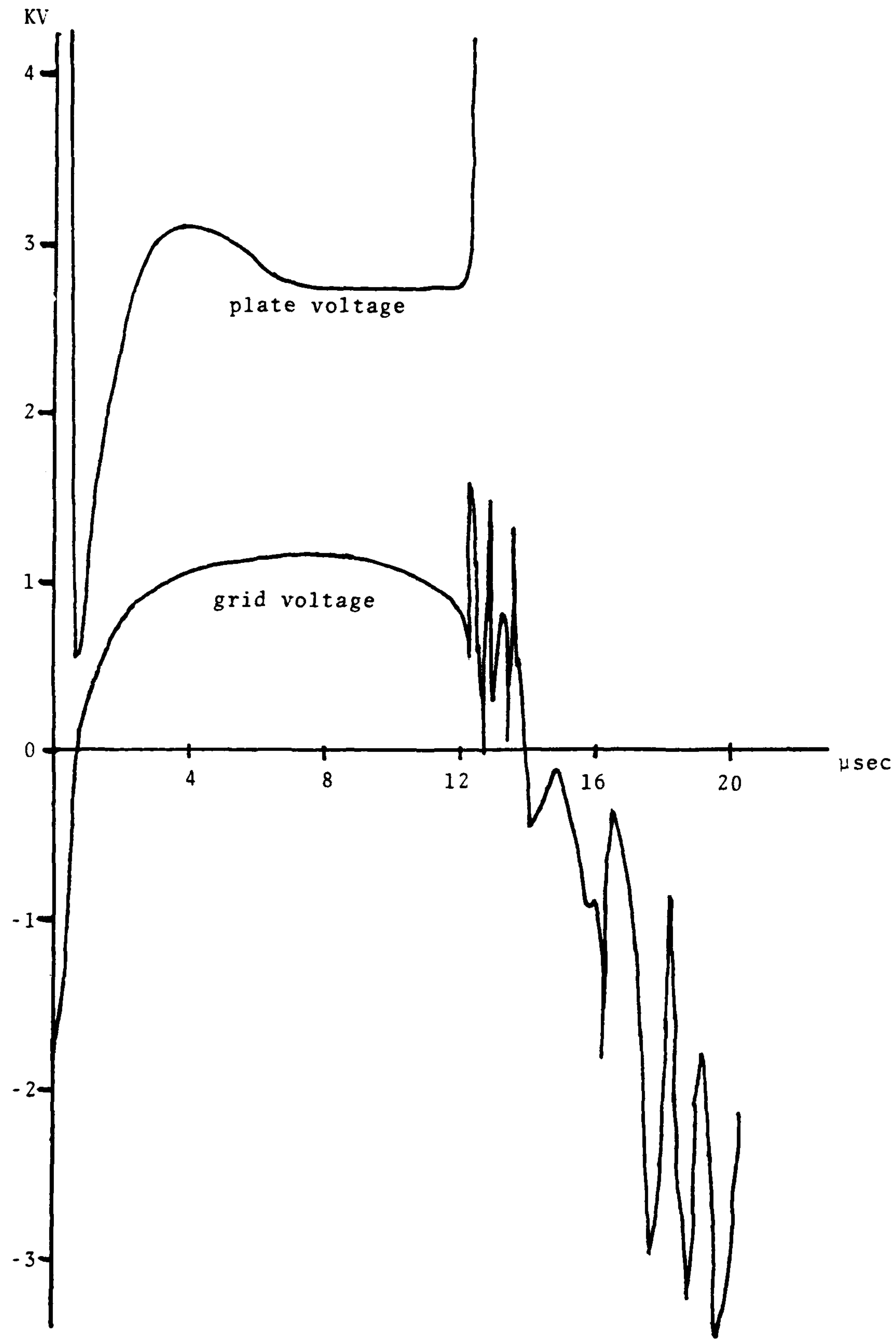

Figure 24. Voltage-Pulse at the Tube Grid and Plate

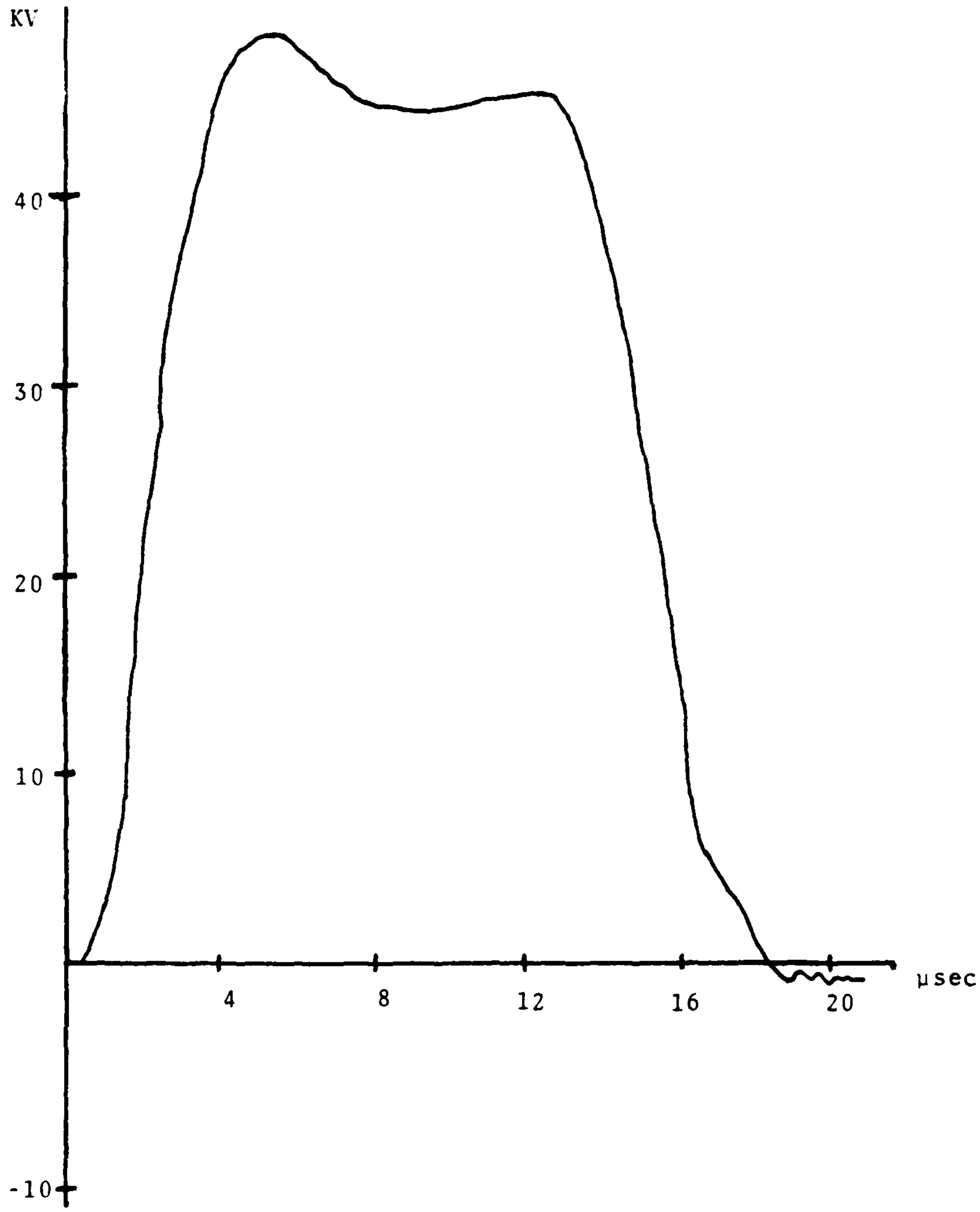

Figure 25. Voltage-Pulse Across the E-Gun Impedance

IV. Conclusions and Recommendations

This study investigated the effects of a pulse-forming network, within a power modulator, operating into non-linear load. The PFN was constructed in modules for varying the pulse widths.

A successful modular PFN design was demonstrated by actual test results. The Rayleigh PFN design had minimum pulse-plateau ripple as modules were added or removed. This low-ripple response was achieved without incorporating mutual inductance into the design. Mutual inductance has been considered indispensible in PFN's, but it is a roadblock for modular construction. Its elimination as a design parameter is the key to realizing the modular PFN. The response of the PFN operating, within the power modulator, into the non-linear load of the power tubes was studied with computer analysis. The modulator was required to deliver a specified voltage-pulse to the electron-beam gun's cathode. The PFN performed well enough for the modulator to accomplish this goal.

The computer test results showed excessive oscillation at the end of the PFN and at the tube grid voltage-pulses. It is significant that they occured as the power tubes turned off. When the voltage at a power tube grid is less than zero, the tube will turn off and thus there will be zero grid current (even when the grid voltage continues to go negative). The tubes turning off have the effect of increasing the PFN's load impedence to several times the matched load it was designed

for, the effect is similar to a transmission line operating into an unmatched load. It was possible to compensate the circuit for this affect, by increasing the inductance of L7, of Figure 21, until an optimum response was obtained. This essentially increases the PFN's characteristic impedance. This is where computer modeling is essential, because various element values can be varied until the desired results are obtained

The purpose of the PFN was to turn on and off the power tubes, not to deliver a perfect voltage or current pulse. Though inefficient it fulfilled this purpose. When the rise and fall times are important and not the pulse shape it is possible to use a PFN to drive a non-linear load.

Further study can be done by actually building the power modulator and comparing actual test results to those obtained by computer analysis. The affect of the oscillations at the end of the grid and PFN pulses on the stability of the modulator can then be determined accurately.

The power modulator stability can be further studied using control theory. The model in Figure 22 can be used to derive a power modulator transfer equation. This equation can be used to determine the circuit stability and to find which circuit elements have the most effect on stability.

This study has shown that it is possible to model a power modulator circuit, which uses power tubes, on a digital computer. The circuit operation can then be analyzed and any corrective adjustments be made before the circuit is constructed.

The techniques verified in this report make it possible to study circuits where the voltages and currents at certain nodes are non-linearly dependent on other nodal voltages and currents.

Bibliography

1. Ball, D.G. and T.R. Burkes. "PFN Design for Time-Varying Loads," IEEE Conference Record of 1978 Thirteenth Pulse Power Modulator Symposium: 156-161 (June 1978).

2. Blinchikoff, H.J. Lightweight Line Pulse. RADC-TR-78-73. Griffiss AFIR, New York: Rome Air Development Center. 1978

3. Bowers, J.C. and S.R. Sedore. SCEPTRE: A Computer Program for Circuit and Systems Analysis. Englewood, New Jersey: Prentice-Hall, Inc., 1971.

4. Glascoe, G.N. and J.V. Labacqz. Pulse Generators. New York: Dover Publications, 1965.

5. Grover, F.W. Inductance Calculations, Working Formulas and Tables. New York: D. Van Nostand Company, Inc., 1946.

6. Machlett Laboratories. ML-7560, ML-8317 Tube Descriptions. Stamford, Connecticut, 1980.

7. O'Loughlin, J.P. Memo for the Record, Hot Cathode Electron Beam Gun Instabilities and Arc-Downs. Air Force Weapons Laboratory, Kirtland Air Force Base, New Mexico, 19 June 1980.

8. O'Loughlin, J.P. Project Engineering, Personal Files. Air Force Weapons Laboratory, Kirtland Air Force Base, New Mexico.

9. O'Loughlin, J.P. Memo for the Record, Computerized Circuit Analysis Method. Air Force Weapons Laboratory, Kirtland Air Force Base, New Mexico, 21 August 1978.

10. Roark, R.M. et al. "Pulse Forming Networks with Time Varying or Non-Linear Loads," IEEE Conference Record of 1978 Thirteenth Pulse Power Modulator Symposium: 46-50 (June 1978).

11. Ryder, J.D. Electronic Engineering Principles. New York: Prentice Hall, 1947.

APPENDIX A

Appendix A

Coil Inductance Calculations

The inductor coils were air coil inductors four and one half inches in diameter, four and three fourths inches long. The coil inductance was calculated using Nagaoko's formula, which is based on the well-known formula for the inductance of a cylinfrical current sheet of infinite length and applies a correction to take account of the effect of the ends (Ref 5: 142-147).

Nagaoko's formula is:

$$L = 0.004\pi^2 a^2 b n^2 k \qquad \text{(A-1)}$$

where

n is the winding density in turns per centimeter

k is the factor that takes into account the effect of the ends

a is the radius of the coil in centimeters

b is the length of the coil in centimeters

Nagaoko gave a table of values for k as a function of the shape ratio 2a/b.

For the designed PFN:

2a = 4.5 inches

b = 4.75 inches

n = 2.75 turns per inch

k = 0.7

After converting to centimeters, these dimensions gave an inductance value of L=12.73μh, which is 11 per cent higher than

the needed value of inductance but desired because the PFN will be fined tuned by adjusting taps on the inductors.

APPENDIX B

Appendix B

Minimizing Coil Coupling

The mutual coupling between two coils can be calculated by visualizing the empty space between the coils as another coil, as shown in Figure 26.

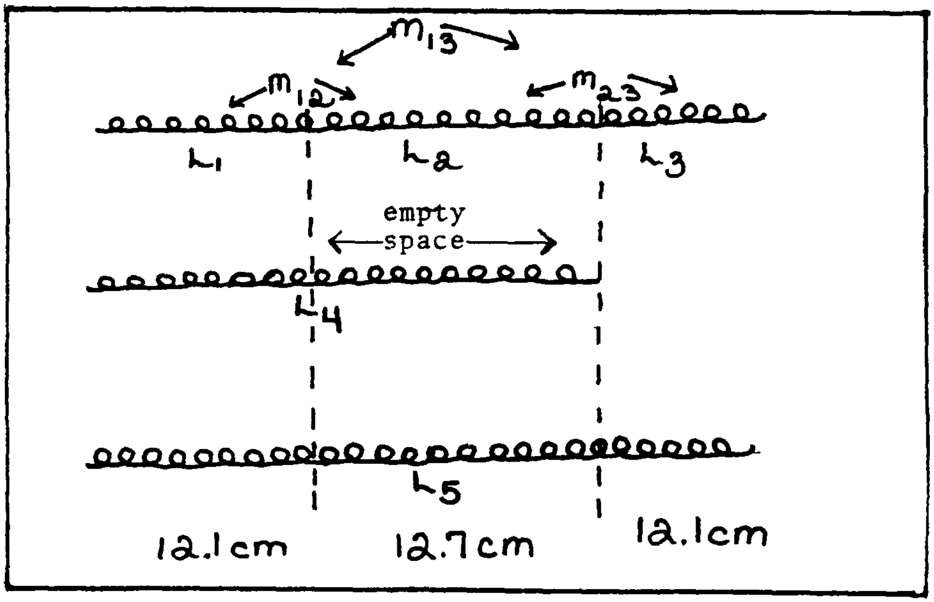

Figure 26. Two Coils Separated by a Space Represented as Three Coils

L_5 is found by

$$L_5 = L_1+L_2+L_3+2M_{12}+2M_{23}+2M_{13} \tag{B-1}$$

L_1 and L_3 are known to be 12.73 ħ, by using Nagaoko's formula (see Appendix A). The coil inductance is found using the coil's physical dimensions. Thus L_5, L_2 and L_4 can be calculated and then M_{12} and M_{23} derived from the results.

L_4 is found by

$$L_4 = L_1+L_2+2M_{12} \tag{B-2}$$

Nagaoko's formula is

$$L = 0.004\Pi^2 a^2 b n^2 k \tag{B-3}$$

The values to use for L_4 are

$a = 5.72$ cm

$b = 24.77$ cm

$n = 1.08$ turns per cm

$k = 0.83$

Then

$$L_4 = 30.97\mu h \tag{B-4}$$

The values to use for L_2 are

$a = 5.72$cm

$b = 12.7$cm

$n = 1.08$ turns per cm

$k = 0.71$

Then

$$L_2 = 13.59\mu h \tag{B-5}$$

Using Equation B-2

$$M_{12} = 2.33\mu h \tag{B-6}$$

from symmetry

$$M_{12} = M_{23} \tag{B-7}$$

The values to use for L_5 are

$a = 5.72$cm

$b = 36.83$cm

$n = 1.08$ turns per cm

$k = 0.88$

Then

$$L_5 = 48.83\mu h \tag{B-8}$$

Using equation B-1

$$M_{13} = 0.23\mu h \tag{B-9}$$

Which is only 1.8 per cent of the coil inductance

The PFN capacitors have an internal inductance. That inductance is considered to be in series with the coil coupling inductance produced by the T equivalent circuit of the PFN inductor coils. The resulting mutual inductance is much smaller than .23μh. Figure 27 shows the transformation of two series coils with a mutual inductance to a T equivalent circuit. If the transformation is true than

between A and C

$$2L_1 = 2L + 2M \tag{B-10}$$

and between A and B

$$L = L_1 + L_2 \tag{B-11}$$

This reduces to

$$L_1 = L + M \tag{B-12}$$

$$L_2 = -M \tag{B-13}$$

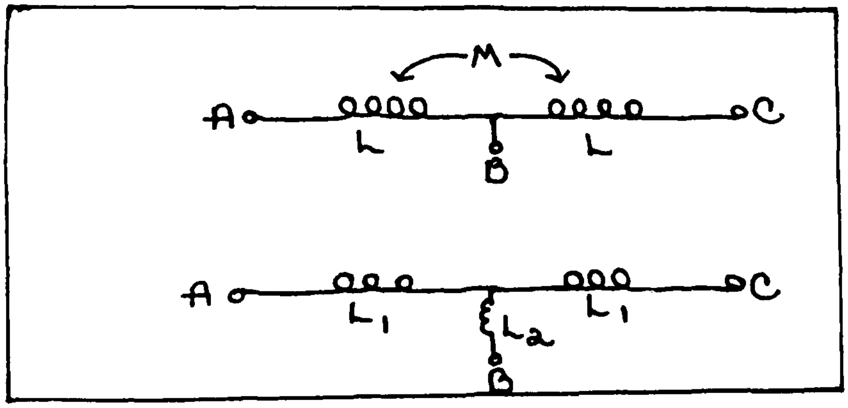

Figure 27. T Equivalent Circuit of Two Series Coils

with

$$L = 12.73\mu h \tag{B-14}$$

$$M = 0.23\mu h \tag{B-15}$$

then

$$L_1 = 12.96\mu h \tag{B-16}$$

$$L_2 = -0.23\mu h \tag{B-17}$$

The resonant frequency of the capacitors is $f = 1.5\ MH_z$. The internal inductance is then found by

$$(2\pi f)^2 = 1/_{L_i C} \tag{B-18}$$

with

$$f = 1.5\ MH_Z \tag{B-19}$$

$$C = 50nf \tag{B-20}$$

then

$$L_i = .225\mu h \tag{B-21}$$

The capacitor's internal inductance, L_i in equation B-21, is in series with the mutual inductance between the coils, L_2 in equation B-17. This series combination reduces the overall mutual inductance to a negligible 0.005μh.

APPENDIX C

Appendix C

SCEPTRE and FORTRAN Programs

The SCEPTRE program model of the Type-E PFN is shown on pages 51 thru 52. The program shown is for all fou modules. On pages 53 thru 54 is the SCEPTRE program model of the Rayleigh PFN. The program shown is for all four modules.

The power modulator FORTRAN model is shown on I 'ges 55 thru 58.

```
[illegible] DESCRIPTION
[illegible]
[illegible] 1•10E-6
[illegible]•10E-6
[illegible],4-[illegible]•10E-6
[illegible]4,5-4•10E-6
L5,[illegible]-5•10E-6
L6,7-[illegible]•10E-6
L7,8-[illegible]•1[illegible]E-6
C1,2-9•50E-9
C2,3-9•50E-9
C3,4-9•50E-9
C4,5-9•50E-9
C5,6-9•50E-9
C6,7-9•50E-9
C7,8-9•50E-9
M12,L1-L2•1.5E-6
M23,L2-L3•1.5E-6
M34,L3-L4•1.5E-6
M45,L4-L5•1.5E-6
M56,L5-L6•1.5E-6
M67,L6-L7•1.2E-6
L8,10-8•16E-6
L9,11-10•10E-6
L10,12-11•10E-6
L11,13-12•10E-6
L12,14-13•10E-6
L13,15-14•10E-6
L14,16-15•12E-6
C8,10-9•50E-9
C9,11-9•50E-9
C10,12-9•50E-9
C11,13-9•50E-9
C12,14-9•50E-9
C13,15-9•50E-9
C14,16-9•50E-9
MA,L8-L9•1.5E-6
MB,L9-L10•1.5E-6
MC,L10-L11•1.5E-6
MD,L11-L12•1.5E-6
ME,L12-L13•1.5E-6
MF,L13-L14•1.2E-6
L15,17-16•16E-6
L16,18-17•10E-6
L17,19-18•10E-6
L18,20-19•10E-6
L19,21-20•10E-6
L20,22-21•10E-6
L21,23-22•12E-6
C15,17-9•50E-9
C16,18-9•50E-9
C17,19-9•50E-9
C18,20-9•50E-9
C19,21-9•50E-9
C20,22-9•50E-9
C21,23-9•50E-9
MG,L15-L16•1.5E-6
MH,L16-L17•1.5E-6
MI,L17-L18•1.5E-6
MJ,L18-L19•1.5E-6
MK,L19-L20•1.5E-6
ML,L20-L21•1.2E-6
..
```

```
2.24-23•10E-6
3.25-24•10E-6
4.26-25•10E-6
 .27-26•10E-6
 .28-27•10E-6
 .29-28•10E-6
S.30-29•10E-6
 .24-9•50E-9
 .25-9•50E-9
4.26-9•50E-9
 .27-9•50E-9
6.28-9•50E-9
 .29-9•50E-9
 S.30-9•50E-9
 ,L22-L23•1.5E-6
 ,L23-L24•1.5E-6
 ,L24-L25•1.5E-6
 ,L25-L26•1.5E-6
 ,L26-L27•1.5E-6
 ,L27-L28•1.2E-6
RL,S-1•15
INITI L CONDITIONS
VC1•10E3
VC2•10E3
VC3•10E3
VC4•10E3
VC5•10E3
VC6•10E3
VC7•10E3
VC8•10E3
VC9•10E3
VC10•10E3
VC11•10E3
VC12•10E3
VC13•10E3
VC14•10E3
VC15•10E3
VC16•10E3
VC17•10E3
VC18•10E3
VC19•10E3
VC20•10E3
VC21•10E3
VC22•10E3
VC23•10E3
VC24•10E3
VC25•10E3
VC26•10E3
VC27•10E3
 C28•10E3
 TPUTS
 RL
 UN CONTROLS
INTEGRATION ROUTINE•IMPLICIT
 TOP TIME•60E-6
 D
```

```
CIRCUIT DESCRIPTION
ELEMENTS
L1,2-1•11E-6
L2,3-2•11E-6
L3,4-3•11E-6
L4,5-4•11E-6
L5,6-5•11E-6
L6,7-6•11E-6
L7,8-7•11E-6
C1,2-9•50E-9
C2,3-9•50E-9
C3,4-9•50E-9
C4,5-9•50E-9
C5,6-9•50E-9
C6,7-9•50E-9
C7,8-9•50E-9
L8,10-5•11E-6
L9,11-10•11E-6
L10,12-11•11E-6
L11.13-12•11E-6
L12.14-13•11E-6
L13.15-14•11E-6
L14.16-15•11E-6
C8,10-9•50E-9
C9,11-9•50E-9
C10,12-9•50E-9
C11.13-9•50E-9
C12.14-9•50E-9
C13.15-9•50E-9
C14.16-9•50E-9
L15.17-16•11E-6
L16.19-17•11E-6
L17,19-18•11E-6
L18.20-19•11E-6
L19,21-20•11E-6
L20,22-21•11E-6
L21,23-22•11E-6
C15,17-9•50E-9
C16,18-9•50E-9
C17,19-9•50E-9
C18,20-9•50E-9
C19,21-9•50E-9
C20,22-9•50E-9
C21,23-9•50E-9
L22,24-23•11E-6
L23,25-24•11E-6
L24,26-25•11E-6
L25,27-26•11E-6
L26,28-27•11E-6
L27,29-28•11E-6
L28,30-29•11E-6
C22,24-9•50E-9
C23,25-9•50E-9
C24,26-9•50E-9
C25,27-9•50E-9
C26,28-9•50E-9
C27,29-9•50E-9
C28,30-9•50E-9
RL,3-1•15
INITIAL CONDITIONS
VC1•10E3
VC2•10E3
..
```

```
C3•10E3
C4•10E3
C5•10E3
C6•10E3
C7•10E3
C8•10E3
C9•10E3
C10•10E3
C11•10E3
C12•10E3
C13•10E3
C14•10E3
C15•10E3
C16•10E3
C17•10E3
C18•10E3
C19•10E3
C20•10E3
C21•10E3
C22•10E3
C23•10E3
C24•10E3
C25•10E3
C26•10E3
C27•10E3
C28•10E3
OUTPUTS
ALL
RUN CONTROLS
INTEGRATION ROUTINE•IMPLICIT
STOP TIME•60E-6
END
```

```
PROGRAM EGUN(INPUT,OUTPUT,TAPE5=INPUT,TAPE6=OUTPUT)
DIMENSION V(20),AT(240),AVG(240),AVP(240),AGC(240),APC(240)
AL=[illegible].64E-6
AC=[illegible]2E-9
VA=50E3
VB=-2E3
VC=5E3
V(1)=VC
V(2)=VC
V(3)=VC
V(4)=VC
V(5)=VC
V(6)=VC
V(7)=VC
V(8)=VB
V(9)=VB
V(10)=VB
V(11)=VB
V(12)=VB
V(13)=VA
V(14)=VA
V(15)=VA
V(16)=VA
V(17)=VA
V(18)=VA
VG=V(12)
VP=V(13)
AI12=0
AI23=0
AI34=0
AI45=0
AI56=0
AI67=0
AI78=0
AI89=0
AI1011=2
AI1314=0
AI1415=0
AI1516=0
DV1=0
DV2=0
DV3=0
DV4=0
DV5=0
DV6=0
DV7=0
DV10=0
DV12=0
DV13=0
DV14=0
DV15=0
DV18=0
AL12=AL
AL23=AL
AL34=AL
AL45=AL
AL56=AL
AL67=AL
AL78=34.83E-6
C110=AC
C210=AC
C310=AC
C410=AC
```

```
      C510=AC
      C610=AC
      C710=AC
      AL1213=20E-6
      AL89=7E-6
      R910=35
      C100=240E-6
      R100=1000
      AL1011=250E-3
      R912=.5
      AL1314=83E-6
      C1415=15E-9
      AL1415=33E-3
      C130=15E-12
      C120=500E-12
      C1213=300E-12
      R1415=3200
      R1518=1
      C180=5.5E-6
      AL1516=5E-6
      R1617=100
      R1319=.5
      V(19)=VA
      TTT=20E-6
      TT=0
      DT=1E-9
      VR=0
      T=0
      SC=0
      PC=0
      I=0
      AIF=0
      GO TO 140
   10 CONTINUE
      DU1=(C110*DU10/DT-AI12+DT*(V(2)-V(1))/AL12)*DT/C110
      V(1)=V(1)+DU1
      DU2=(C210*DU10/DT+AI12-AI23+DT*(V(1)-V(2))/AL12
     C+DT*(V(3)-V(2))/AL23)*DT/C210
      V(2)=V(2)+DU2
      DU3=(C310*DU10/DT+AI23-AI34+DT*(V(2)-V(3))/AL23
     C+DT*(V(4)-V(3))/AL34)*DT/C310
      V(3)=V(3)+DU3
      DU4=(C410*DU10/DT+AI34-AI45+DT*(V(3)-V(4))/AL34
     C+DT*(V(5)-V(4))/AL45)*DT/C410
      V(4)=V(4)+DU4
      DU5=(C510*DU10/DT+AI45-AI56+DT*(V(4)-V(5))/AL45
     C+DT*(V(6)-V(5))/AL56)*DT/C510
      V(5)=V(5)+DU5
      DU6=C610*DU10/DT+AI56-AI67+DT*(V(5)-V(6))/AL56
     C+DT*(V(7)-V(6))/AL67*DT/C610
      V(6)=V(6)+DU6
      DU7=(C710*DU10/DT+AI67-AI78+DT*(V(6)-V(7))/AL67
     C+DT*(V(8)-V(7))/AL78)*DT/C710
      V(7)=V(7)+DU7
      V(8)=(AI78+V(7)*DT/AL78-AI89+V(9)*DT/AL89)/(DT/AL78+DT/AL89)
      V(9)=(V(10)/R910+V(12)/R912+AI89+V(8)*DT/AL89)
     C/(1/R910+1/R912+DT/AL89)
      DU10=((V(9)-V(10))/R910-V(10)/R100+C110*DU1/DT
     C+C210*DU2/DT+C310*DU3/DT+C410*DU4/DT+C510*DU5/DT+C610*DU6/DT
     C+C710*DU7/DT-AI1011+DT*(V(11)-V(10))/AL1011)/(C110/DT+C210/DT
     C+C310/DT+C410/DT+C510/DT+C610/DT+C710/DT+C100/DT)
      V(10)=V(10)+DU10
      DU12=(C1213*DU13/DT-GI(UG,UP)+(V(9)-V(12))/R912)
```

```
     C (C1213/DT+C120/DT)
      V(12)=V(12)+DV12
      DV13=(C1213*DV12/DT-PI(VG,VP)+(V(19)-V(13))/R1319)
     C /(C1213/DT+C130/DT)
      V(13)=V(13)+DV13
      V(19)=(V(13)/R1319+AI1314+V(14)*DT/AL1314)
     C /(1/R1319+DT/AL1314)
      DV14=((V(15)-V(14))/R1415+C1415*DV15/DT+AI1415
     C+DT*(V(15)-V(14))/AL1415-AI1314
     C+DT*(V(19)-V(14))/AL1314)*DT/C1415
      V(14)=V(14)+DV14
      DV15=((V(14)-V(15))/R1415+(V(18)-V(15))/R1518+C1415*DV14/DT
     C+AI1516+DT*(V(16)-V(15))/AL1516-AI1415
     C+DT*(V(14)-V(15))/AL1415)*DT/C1415
      V(15)=V(15)+DV15
      V(16)=(V(17)/R1617-AI1516+V(15)*DT/AL1516)/(1/R1617+DT/AL1516)
      DV18=(V(15)-V(18))/R1518*DT/C180
      V(18)=V(18)+DV18
      AI12=AI12+DT*(V(1)-V(2))/AL12
      AI23=AI23+DT*(V(2)-V(3))/AL23
      AI34=AI34+DT*(V(3)-V(4))/AL34
      AI45=AI45+DT*(V(4)-V(5))/AL45
      AI56=AI56+DT*(V(5)-V(6))/AL56
      AI67=AI67+DT*(V(6)-V(7))/AL67
      AI78=AI78+DT*(V(7)-V(8))/AL78
      AI89=AI89+DT*(V(8)-V(9))/AL89
      AI1011=AI1011+DT*(V(10)-V(11))/AL1011
      AI1314=AI1314+DT*(V(14)-V(19))/AL1314
      AI1415=AI1415+DT*(V(15)-V(14))/AL1415
      AI1516=AI1516+DT*(V(16)-V(15))/AL1516
      VG=V(12)
      VP=V(13)
      PC=PI(VG,VP)
      GC=GI(VG,VP)
      VR=V(15)-V(14)
      R1415=R(VR)
      AIR=VR/R1415
      IF(T.GE.TTT)GO TO 50
      IF(T.GE.TT)GO TO 140
      T=T+DT
      GO TO 10
  140 CONTINUE
      WRITE(6,20)(T,V(8),V(14),V(9),V(10),VR,AIR)
      I=I+1
      AT(I)=T
      AVG(I)=V(12)
      AVP(I)=V(13)
      AGC(I)=GC
      APC(I)=PC
   20 FORMAT(1(1X,E14.3,4X,E14.3,4X,E14.3,4X,E14.3,4X,E14.3
     C,4X,E14.3,4X,E14.3))
      TT=1E-7+TT
      GO TO 10
   50 CONTINUE
      WRITE(6,21)
   21 FORMAT(1H0)
      DO 60 J=1,I
      WRITE(6,20)(AT(J),AVG(J),AGC(J),AVP(J),APC(J))
   60 CONTINUE
      END
      FUNCTION GI(VG,VP)
      PIE=3.141597
      IF(VG)110,110,120
```

```
110 GI=0
    RETURN
120 A=.0432*UG
    B=.038*UG
    X=3.332*UG
    Y=X-UP
    Z=UP-X-1.25
    GI=(B-.0192*UP)/PIE*(ATAN(Y)+PIE/2)
   C+(A-.00254*UP)/PIE*(ATAN(Z)+PIE/2)
    GI=4.*GI
    IF(GI.GE.0)GO TO 130
    GI=0
130 CONTINUE
    RETURN
    END
    FUNCTION PI(UG,UP)
    IF(UP.GE.0)GO TO 200
    PI=0
    RETURN
200 CONTINUE
    PIE=3.141597
    A=.22*UG
    X=3.6*UG-300
    Y=X-UP
    Z=UP-X
    PI=.0714*UP/PIE*(ATAN(Y)+PIE/2)
   C+(A+.0034*UP)/PIE*(ATAN(Z)+PIE/2)
    PI=4.*PI
    IF(PI.GE.0)GO TO 210
    PI=0
210 CONTINUE
    RETURN
    END
    FUNCTION R(UR)
    IF(UR.LE.0)GO TO 310
    IF(UR.GE.1520)GO TO 300
    R=1/(.00727*UR**.5)
    R=3200*R/(3200+R)
    RETURN
300 CONTINUE
    R=UR/(700*(1-EXP(-(UR-1000)*.00185)))
    R=3200*R/(3200+R)
    RETURN
310 CONTINUE
    R=3200
    RETURN
    END
```

APPEDIX D

Appendix D

Power Triodes and E-Gun Impedence Subroutines

The grid and plate currents, being functions of both the grid and plate voltages, were determined by function subroutines. Linear equations were derived to closely approximate the non-linear relationship (obtained from the tube characteristic curves) between the tube voltages and currents (Ref 6).

As seen in Figure 28, the grid current vs. plate voltage, for a constant grid voltage, can be approximated by two lines. This piece-wise linear relationship can be expressed by the equation

$$i_{grid} = [a_1 - 0.0192z][\tan^{-1}(x_b - x) + \Pi/2]/\Pi +$$

$$[a_2 - 0.00264x][\tan^{-1}(x - x_b - 1.25) + \Pi/2]/\Pi \qquad \text{(D-1)}$$

where

a_1 is the y intercept of line A in amps

a_2 is the y intercept of line B in amps

x_b is the intercept of line A and line B in volts

x is the plate voltage in volts

a_1, a_2, and x_b orientate the current function to the operating grid voltage and are expressed by the linear equations

$$a_2 = 0.0432 * V_{grid} \text{ in volts} \qquad \text{(D-3)}$$

$$a_1 = 0.098 * V_{grid} \text{ in volts} \qquad \text{(D-4)}$$

$$x_b = 3.332 * V_{grid} \text{ in volts} \qquad \text{(D-5)}$$

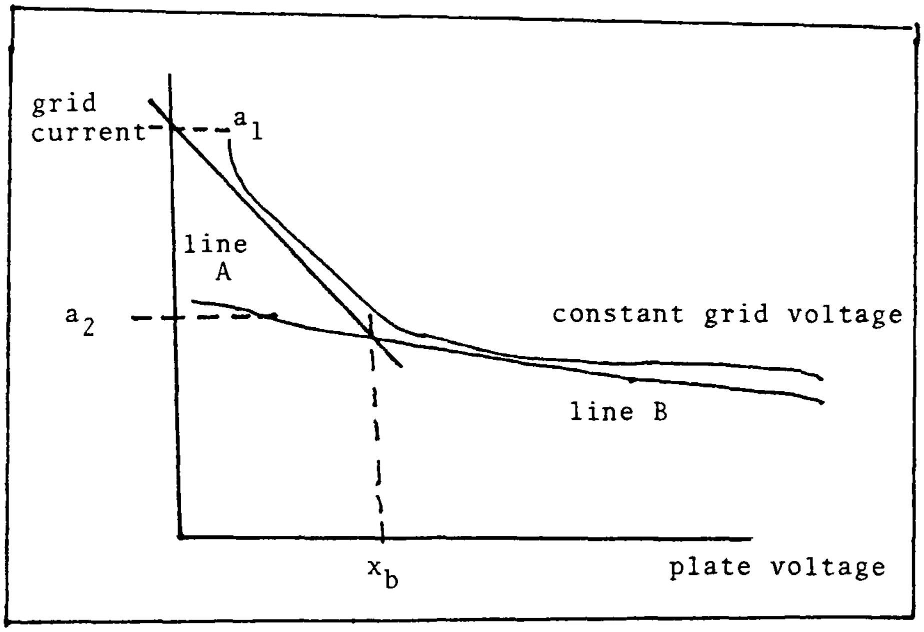

Figure 28. Piece-noise Approximation of Grid Current Function

A comparison of the actual grid current vs. plate voltage, for a constant grid voltage, curves with curves derived from the grid current subroutine is shown in Figure 29.

The plate current subroutine was derived in the same manner as the grid current subroutine. The plate current as a function of grid voltage and plate voltage can be expressed as

$$i_{plate} = [0.0714\ x/\pi][\tan^{-1}(0006(x_b - x) + \pi/2] + [a_2 + 0.0034x][\tan^{-1}(x - x_b - 0.6) + \pi/2]\ /\pi \quad \text{(D-6)}$$

where

a_2 = .22 * V_{grid} in volts

x_b = 3.6 * V_{grid} - 3[illegible]0 in volts

x = V plate in volts

A comparison of the actual plate current vs. plate voltage,

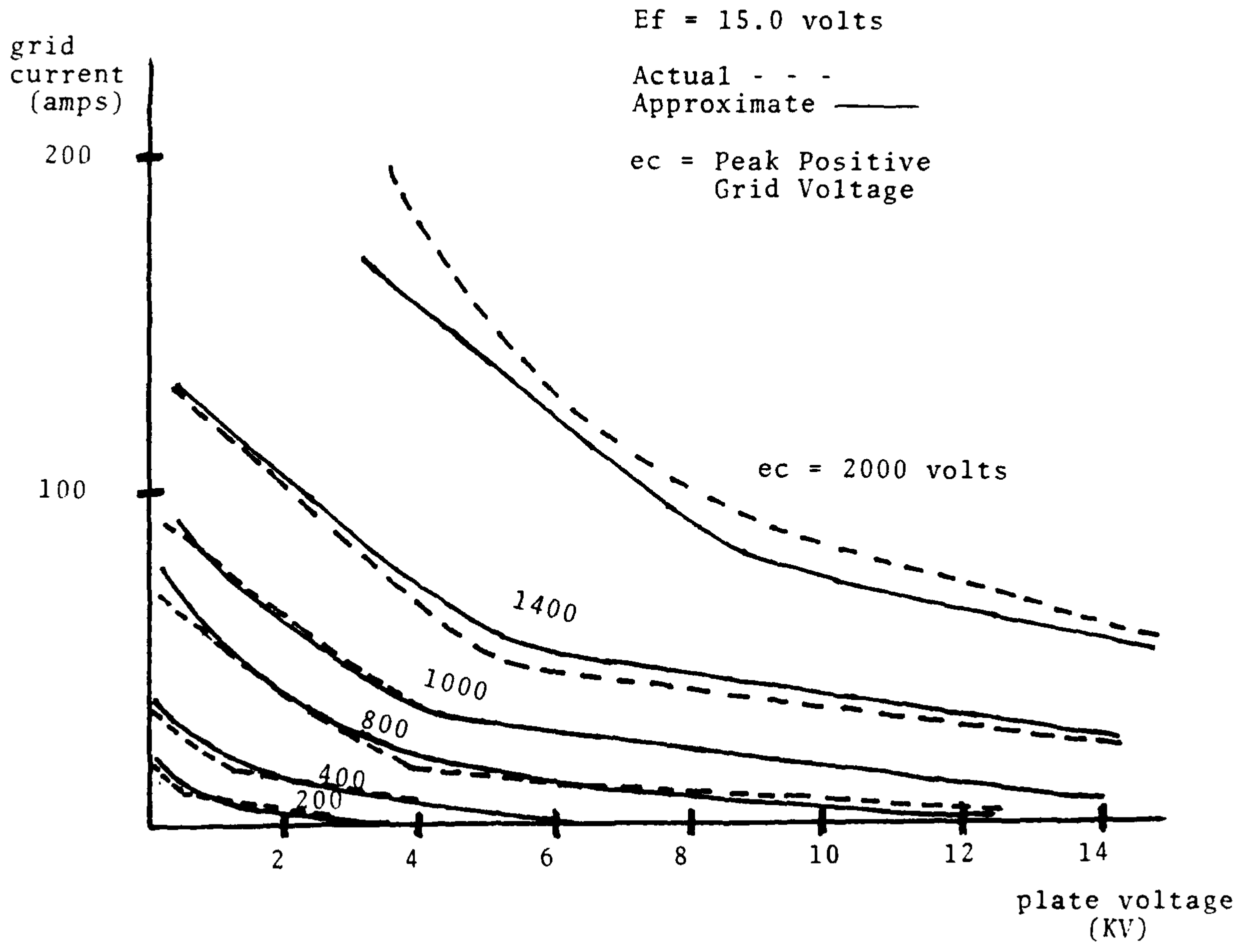

Figure 29. Approximation of Grid Current

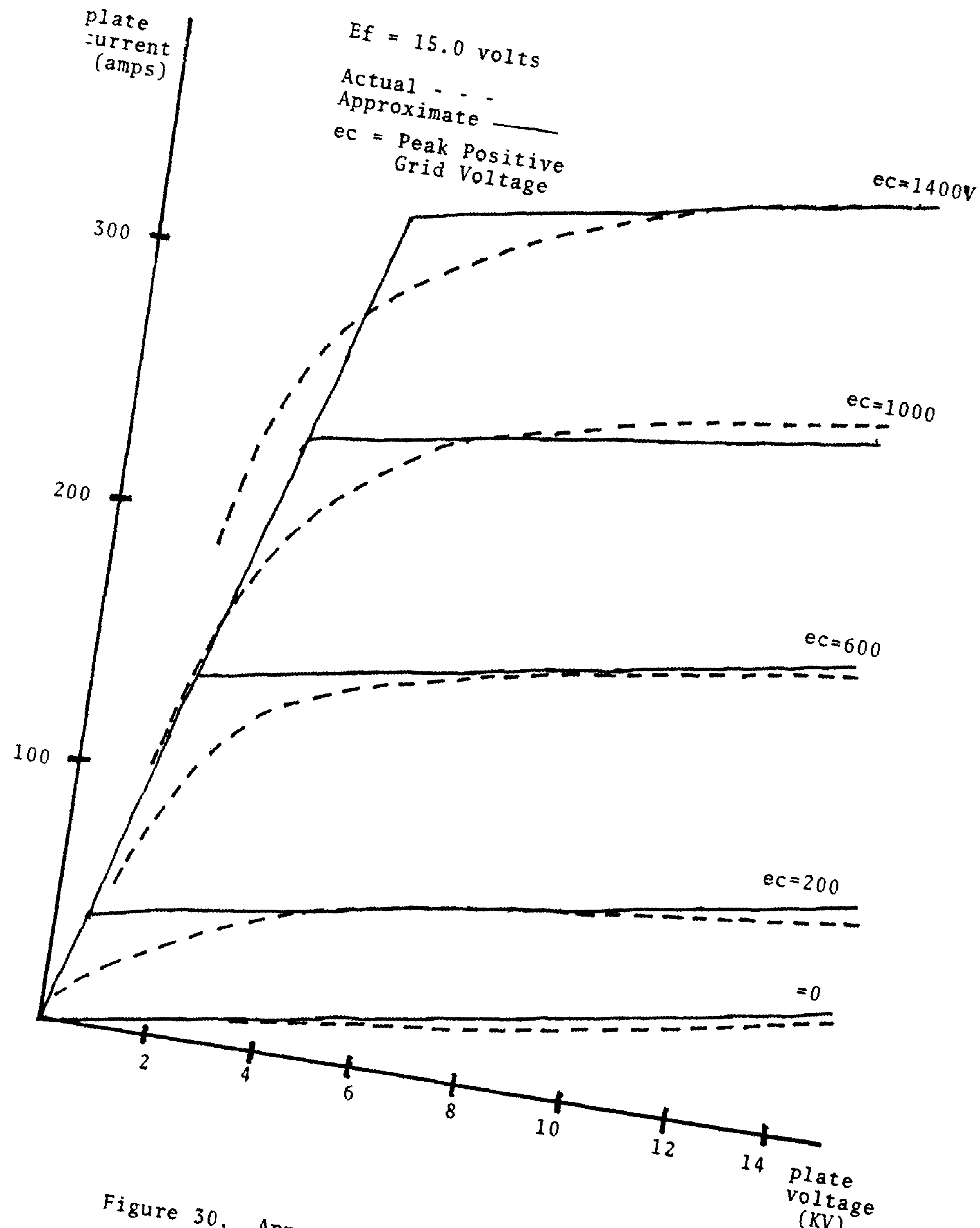

Figure 30. Approximation of Plate-Current.

for a constant grid voltage, curves with curves derived from the plate current subroutine is shown in Figure 30.

The E-gun impedence was modeled first as a constant and then as an emission limited impedence. For emission limiting the current was limited by a function subroutine which determined an appropriate value of resistance as a function of the impedence voltage.

Below an E-gun voltage of zero volts the space-charge effect was dominate, and the current was proportional to the three-halves power of the applied voltage (Ref 9:64-69). The current was expressed by the equation

$$I = KV^{3/2} \text{ amps} \tag{D-7}$$

where

K is a tube constant

V is the applied voltage

Above 2100 volts the current was limited to 700 amps due to emission limiting at the cathode. A subroutine was derived to express the E-gun resistance as a function of the applied voltage for a smooth current transition.

Below 1500 volts the current was

$$I = 0.00727 * V^{3/2} \text{ amps} \tag{D-8}$$

so the E-gun impedence below 1500 volts was

$$R = 1/(0.00727 * V^{1/2}) \text{ ohms} \tag{D-9}$$

Above 1500 volts the current was

$$I = 700 * (1 - \varepsilon^{-(VR-1000)*.00185}) \text{ amps} \tag{D-10}$$

So the E-gun impedence above 1500 volts was

$$R = VR/(700 *(1 - \varepsilon^{-(VR-1000)*.00185}) \text{ ohms} \quad (D-11)$$

Together these equations gave a smooth current transition, seen in Figure 31, as the E-gun voltage increased from 0 to 50KV.

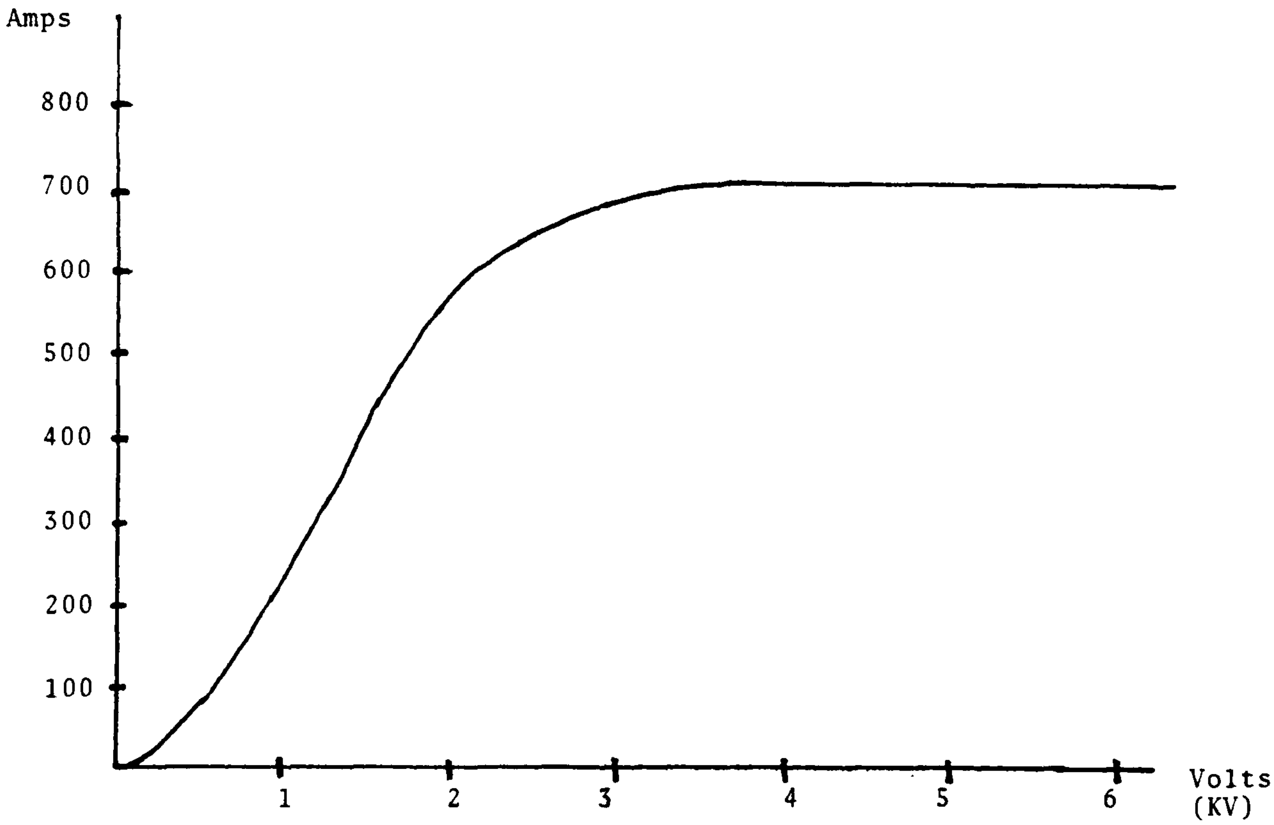

Figure 31. E-gun Current as a Function of Applied Voltage

Vita

Edward Jacob Keefer, Jr. was born on 9 June 1957 in Valparaiso, Florida. He graduated from high school in Niceville, Florida in 1975 and attended Mississippi State University from which he received the degree of Bachelor of Science in Electrical Engineering in August 1979. Upon graduation he received a commission in the United States Air Force through the ROTC program. His initial duty assignment was to the School of Engineering, Air Force Institute of Technology, Wright-Patterson Air Force Base, Ohio in August 1979.

Permanent Address: 224 E 14th St.
Berwick, PA 18603

UNCLASSIFIED

SECURITY CLASSIFICATION OF THIS PAGE (When Data Entered)

REPORT DOCUMENTATION PAGE

READ INSTRUCTIONS BEFORE COMPLETING FORM

1. REPORT NUMBER
AFIT/GE/EE/81M-4 ✓

2. GOVT ACCESSION NO.
AD-A100 797

3. RECIPIENT'S CATALOG NUMBER

4. TITLE (and Subtitle)
EFFECTS OF A PULSE-FORMING NETWORK OPERATING INTO A NON-LINEAR LOAD

5. TYPE OF REPORT & PERIOD COVERED
MS THESIS

6. PERFORMING ORG. REPORT NUMBER

7. AUTHOR(s)
Edward Jacob Keefer, Jr., 2d LT, USAF

8. CONTRACT OR GRANT NUMBER(s)

9. PERFORMING ORGANIZATION NAME AND ADDRESS
School of Engineering
Air Force Institute of Technology (AFIT)
Wright-Patterson AFB OH 45433

10. PROGRAM ELEMENT, PROJECT, TASK AREA & WORK UNIT NUMBERS

11. CONTROLLING OFFICE NAME AND ADDRESS

12. REPORT DATE
15 March 1981

13. NUMBER OF PAGES
73

14. MONITORING AGENCY NAME & ADDRESS(if different from Controlling Office)

15. SECURITY CLASS. (of this report)
UNCLASSIFIED

15a. DECLASSIFICATION/DOWNGRADING SCHEDULE

16. DISTRIBUTION STATEMENT (of this Report)
Approved for public release; distribution unlimited.

17. DISTRIBUTION STATEMENT (of the abstract entered in Block 20, if different from Report)

18. SUPPLEMENTARY NOTES
Approved for public release; IAW AFR 190-17
1 JUN 1981
Fredric C. Lynch
FREDRIC C. LYNCH, Major, USAF
Director of Public Affairs

19. KEY WORDS (Continue on reverse side if necessary and identify by block number)
pulse power
non-linear load
pulse-forming network
electron-beam gun
power modulator

20. ABSTRACT (Continue on reverse side if necessary and identify by block number)

The power modulator of an electron-beam gun was computer modeled to investigate the performance of a pulse-forming network (PFN). The PFN was designed for a constant matched load but operated into non-linear load.

The power modulator's operation consisted of: pulsing the electron-beam gun's cathode to a negative 220KV, thru a pulse transformer, by a 50KV hard-tube pulser, this pulser was switched by four parallel power triodes, which were driven by a line-type pulser or PFN. The triodes, the PFN's load, exhibited

DD FORM 1 JAN 73 1473 EDITION OF 1 NOV 65 IS OBSOLETE

UNCLASSIFIED

SECURITY CLASSIFICATION OF THIS PAGE (When Data Entered)

a non-linear impedance dependent on their grid and plate voltages. The computer model was used to examine the effects of the non-linear load of the power tubes on the PFN.

The PFN was constructed in four; 12KV, 10μsec modules. It was possible to add or remove these modules from the PFN to change the pulse width in 10μ sec steps. This modular PFN design was first investigated using a digital computer model and then built and tested for a constant load. Then the effect of operating into a non-linear load was examined by modeling the PFN within the power modulator.

END

DATE
FILMED
7-81

DTIC